Naval Research Laboratory
Washington, DC 20375-5320

NRL/MR/6180--93-7310

Methanol Pan Fires in an Enclosed Space: Effect of Pressure and Oxygen Concentration

J.L. Bailey, F.W. Williams, and P.A. Tatem

Navy Technology Center for Safety and Survivability
Chemistry Division

March 24, 1993

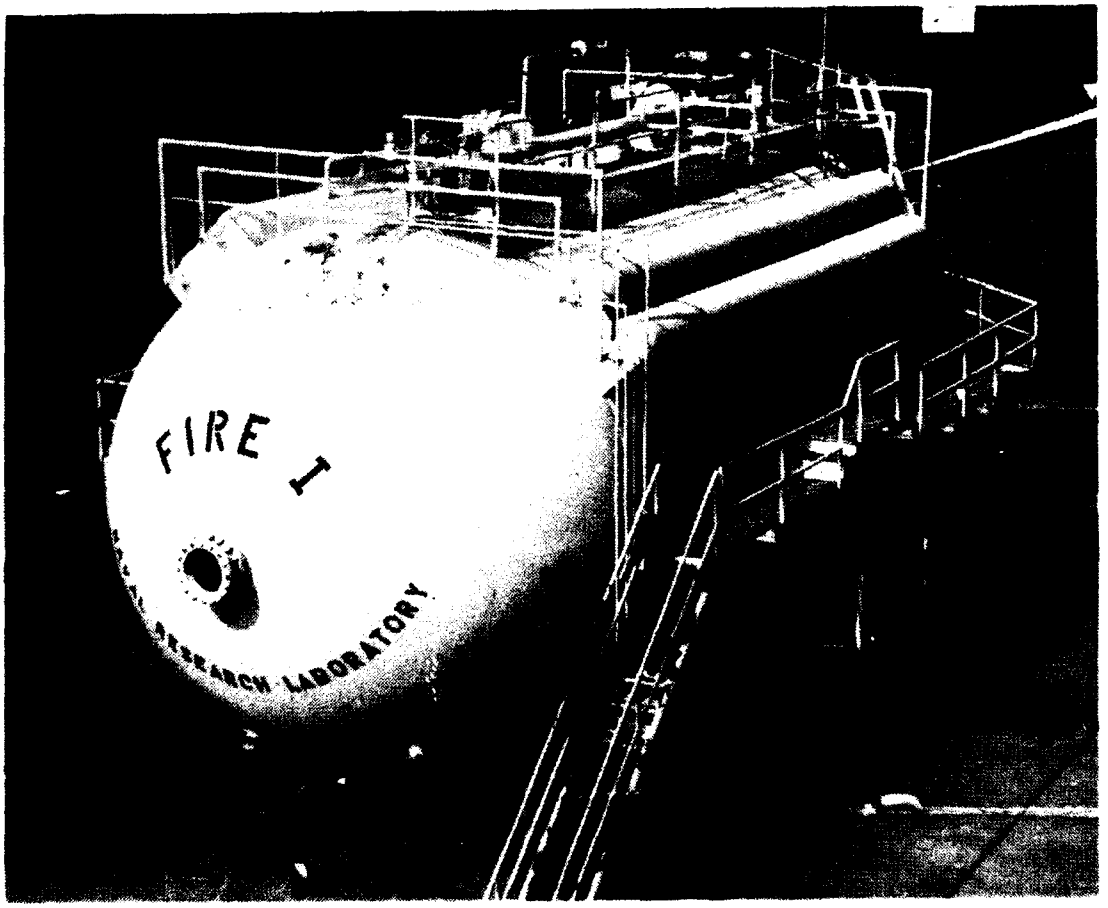

Approved for public release; distribution unlimited.

REPORT DOCUMENTATION PAGE

Form Approved
OMB No. 0704-0188

1. AGENCY USE ONLY (*Leave Blank*)	2. REPORT DATE	3. REPORT TYPE AND DATES COVERED
	March 24, 1993	

4. TITLE AND SUBTITLE

Methanol Pan Fires in An Enclosed Space: Effect of Pressure and Oxygen Concentration

5. FUNDING NUMBERS

OM&N

6. AUTHOR(S)

J.L. Bailey, F.W. Williams and P.A. Tatem

7. PERFORMING ORGANIZATION NAME(S) and ADDRESS(ES)

Naval Research Laboratory
Washington, DC 20375-5320

8. PERFORMING ORGANIZATION REPORT NUMBER

NRL/MR/6180--93-7310

9. SPONSORING/MONITORING AGENCY NAME(S) AND ADDRESS(ES)

Naval Sea Systems Command
Department of the Navy
Washington, DC 20362-5101

10. SPONSORING/MONITORING AGENCY REPORT NUMBER

11. SUPPLEMENTARY NOTES

12a. DISTRIBUTION/AVAILABILITY STATEMENT

Approved for public release; distribution unlimited.

12b. DISTRIBUTION CODE

13. ABSTRACT (*Maximum 200 words*)

A series of fire tests was conducted in FIRE I, a large-scale pressurizable fire test chamber, to investigate the effect of pressure and oxygen concentration on methanol pan fires. As the oxygen concentration decreased from 21 vol-% to 13.5 vol-% throughout the experiments, the mass loss rate linearly decreased from 10 kg/hr to 6.6 kg/hr. Below 13.5 vol-% oxygen concentration, the mass loss rate rapidly declined. The fire self-extinguished when the oxygen concentration level approached 12 vol-%. An increase in initial chamber pressure from 14.7 psi to 23.9 psi (at 21 vol-% initial oxygen concentration) increased the burning rate by 34%. Experiments are planned at combinations of higher than ambient pressures and lower than ambient oxygen concentrations in order to quantify the combined effect of these variables on the mass loss rate of methanol. Experiments are also planned to determine the effect of pressure and oxygen concentration on the burning rates of other fuels.

14. SUBJECT TERMS

Burning rate
Pressure
Oxygen Concentration
Enclosed Spaces
Pan Fires

15. NUMBER OF PAGES

56

16. PRICE CODE

17. SECURITY CLASSIFICATION OF REPORT	18. SECURITY CLASSIFICATION OF THIS PAGE	19. SECURITY CLASSIFICATION OF ABSTRACT	20. LIMITATION OF ABSTRACT
UNCLASSIFIED	UNCLASSIFIED	UNCLASSIFIED	UL

NSN 7540-01-280-5500

Standard Form 298 (Rev. 2-89)
Prescribed by ANSI Std 239-18
298-102

CONTENTS

INTRODUCTION.....1

EXPERIMENTAL CONFIGURATION.....1

EXPERIMENTAL PROCEDURE.....2

RESULTS.....3

CONCLUSION.....6

REFERENCES.....6

METHANOL PAN FIRES IN AN ENCLOSED SPACE: EFFECT OF PRESSURE AND OXYGEN CONCENTRATION

INTRODUCTION

Pressure and oxygen concentration of the surrounding environment are among the parameters which affect the burning rate of a combustible. Since pressure and oxygen concentration can be controlled within a submarine's atmosphere, it should be possible to manipulate these two variables so as to minimize the fire potential. Therefore, as a step toward quantifying the effect of varying pressure and oxygen concentration on fire, several series of large scale fire tests were conducted. The burning rate of a methanol pan fire was measured within the enclosed environment of FIRE I [1], a large-scale pressurizable fire test chamber, at various oxygen concentrations and initial chamber pressures. The initial chamber pressure was varied from 14.7 psia to 23.9 psia. Oxygen concentrations varied from 21 vol-% to 12 vol-% throughout the experiments.

The normal configuration of FIRE I includes a lower and an upper grid-type steel deck. The experiments concerning the variation in pressure and oxygen concentration were conducted without the upper deck in place. Before the test series was concluded, experiments at 21 vol-% and 14.7 psi (1 atm) were conducted with the deck in the chamber to determine its effect.

EXPERIMENTAL CONFIGURATION

A 0.5 m diameter fire pan was located 0.56 m (22 in.) above the lower deck level in the center of FIRE I, a 324-m^3 (11,442-ft^3) pressurizable chamber [1]. The liquid supply system allowed for measurement of methanol loss (burning rate) while keeping the fuel surface level with the lip of the pan. A Sartorius scale, model IB16000S, was used to measure the fuel loss rate. The fuel system is discussed in more detail in reference 1.

In addition to measuring burning rate, chamber gas composition was analyzed at several locations using Beckman 755 oxygen analyzers and Beckman carbon dioxide and carbon monoxide 865 infrared analyzers. There were sample points located in the forward (fwd) end, 1.1 m (43 in.) from the top, and in the aft end, 3.2 m (126 in.) and 1.1 m (43 in.) from the top. These three measurements were averaged to give the average oxygen concentration in the chamber. Chamber pressure was monitored throughout all the experiments using two 0-50 psia Validyne P24 pressure transducers. Note that due to

Manuscript approved January 28, 1993.

the reorientation of FIRE I at the Chesapeake Bay Detachment (CBD), the former "north" and "south" designations in reference 1 will now be referred to as "fwd" and "aft", respectively.

Detailed temperature measurements of the chamber interior atmosphere were made during these experiments using two thermocouple arrays. The "fixed" array was constructed in the aft end of the chamber by stringing cables between the weld ring at 0.76 m (2.5 ft) vertical intervals (Fig. 1). A total of 34 thermocouples were placed on 0.76 m (2.5 ft) horizontal intervals. A "movable" array was constructed in two parts; one section was used in the upper part of the chamber while the other was placed directly below it in the lower section (Figs. 2 and 3). The upper and lower sections of the movable array contained 28 and 25 thermocouples, respectively. The thermocouples were fiberglass sheathed type K thermocouples (20 and 24 gauge). Experiments were repeated with the movable array in different locations in order to map the temperature distribution within the chamber as a function of time.

Temperatures were also measured using permanent fwd and aft thermocouple arrays [1]. Each array consists of 10 thermocouples mounted from top to bottom along a vertical support. The aft permanent array is visible in the background of Figs. 1 through 3. There is a corresponding permanent array located in the fwd end of the chamber.

EXPERIMENTAL PROCEDURE

The eighteen experiments which will be discussed are listed in Table 1. The test names were derived from the type of fuel, date of test, and number of tests done per day. For example, M423B is the name of the second (B) Methanol test done on April 23. The letter designations under the "movable thermocouple array location" column refer to the locations shown in Fig. 4.

The same test scenario was followed for each of the Set 1 tests which had an initial interior environment of 1 atm pressure and 21 vol-% oxygen concentration. The fuel system was charged with methanol, and then the chamber was sealed. Baseline data were collected for 5 min before the fuel was ignited by an electric spark controlled remotely. The fire continued to burn for 1 hr and was then extinguished by covering the fuel pan. Data were collected during the entire 1 hr burn time.

The reduced oxygen atmosphere for the Set 2 tests was achieved by introducing nitrogen into the chamber after it had been sealed. Mixing fans inside the chamber were kept running during this time to insure that the interior was well mixed. Once the oxygen concentration was down to the desired level, the nitrogen addition was stopped, and the chamber was depressurized to 1 atm. Baseline data were again collected for 5 min before the fuel was ignited. Data continued to be collected as the fire was allowed to burn until it self-extinguished. During the M425B test, the chamber was

depressurized to almost 1 atm after 1 hr of burning. The chamber was immediately resealed and the fire was allowed to burn until it self-extinguished.

An air compressor was used to raise the interior pressure of the chamber for the Set 3 experiments. Once the desired pressure was reached, the air addition was stopped, and the 5 min baseline data collection began. The fuel was ignited and data were collected for the next 60 min, at which time the fire was extinguished.

The upper grid-type steel deck was removed prior to conducting Set 1 through Set 3 experiments, but was replaced for the Set 4 experiments. This deck, which separates the upper and lower sections of the chamber, is shown in Fig. 2. All of the Set 4 experiments were performed with an initial oxygen concentration of 21 vol-% and 1 atm pressure. The test procedures were identical to Set 1.

RESULTS

The mass loss rates for the Set 1 experiments as a function of time are shown in Figs. 5 through 7. The location of the movable thermocouple array had no effect on the mass loss rate of the fuel. Oxygen concentrations and pressure data for these experiments are given in Figs. 8 through 10 and 11 through 13, respectively.

The mass loss rates for M425A, M425B, M430A, and M430B are shown in Fig. 14. M425A was chosen as a representative test from the first set of experiments. The higher the initial oxygen concentration, the higher the initial burning rate. This order was maintained throughout the experiments as the mass loss rates decreased with time. This decrease corresponded to the decrease in oxygen concentration of the chamber interior, as shown in Fig. 15. The mass loss rates for M425B after the depressurization at 1 hr burn time, and for M430A and M430B after 1 hr burn time are presented in Fig. 16. M425A is not included as the fire was extinguished after 1 hr. Reliabile mass loss rate data for M425B could not be obtained until the fuel supply system had re-equilibrated after the chamber depressurization. The corresponding oxygen concentrations are given in Fig. 17. Note that the initial burning rate for M425A was 10 kg/hr. This is approximately the value reported in the literature for a 0.5 m diameter methanol pan fire burning in the open [2].

It is well known that both temperature and pressure affect the burning rate [3]. However, the differences in these variables between the four tests and between the start and finish of the individual experiments are small as can be seen in Figs. 18 through 21. The maximum difference in the average chamber interior temperature, as defined by the permanent vertical thermocouple arrays at each end of the chamber [1], was approximately 20°C (Fig. 19). Figures 5, 6 and 22 show that this difference in temperature does not significantly affect the mass loss rate. It will be shown

later that the pressure differences are not of significant magnitude either. Therefore, it is reasonable to plot mass loss rate versus oxygen concentration for the individual tests even though it is known that both the interior temperature and pressure increased slightly with time. Figure 23 shows a linear correlation between mass loss rate and oxygen concentration between 21 vol-% and 13.5 vol-%. Mass loss rate dropped from 10 kg/hr at 21 vol-% to 6.6 kg/hr at 13.5 vol-%. Below 13.5 vol-% oxygen concentration, the mass loss rate rapidly declined until the fire self-extinguished at approximately 12 vol-%. There was very good reproducibility between the three reduced oxygen experiments, M425B, M430A, and M430B. M425A was the only test plotted as a representative of Set 1. It is obvious that the other tests from this set would fall on the same line, as the mass loss rates for all of the tests were almost identical (Figs. 5 through 7), as were the oxygen concentrations as shown in Figs. 8 through 10.

There was very little evidence of incomplete combustion even when very near self-extinguishment. Figure 24 shows that the CO/CO2 ratio remained very small throughout the three experiments which burned until self-extinguishment.

There were over 200 locations monitored for temperature by the movable array alone. Therefore average temperatures of different horizontal cross-sections, as defined by the cross pieces of the movable array, were calculated and used for comparison. Figures 25 through 31 show seven horizontal levels, approximately 0.76 m (30 in.) apart, beginning 0.36 m (14 in.) from the lower deck. Even though the average initial temperatures were lower for the experiments in Set 1, the rate of temperature increase was greater than the reduced oxygen tests. This is consistent with the higher mass loss rates obtained during the Set 1 experiments. From these plots it is evident that there was significant stratification with respect to interior gas temperature. The temperatures near the bottom of the chamber remained near ambient, while the temperatures near the top of the chamber reached 65°C.

Most of the combustion heat is lost to the steel walls of the chamber. If FIRE 1 were adiabatic, the temperature rise at the end of 1 hr of burning in an initial environment of 21 vol-% oxygen concentration and 1 atm pressure would be approximately 450°C. The actual increase in temperature was less than 50°C even in the warmest portion of the chamber.

The mass loss rates for the experiments in Set 3 (M502A, M503A, and M514A) are shown in Fig. 32. M425A is also plotted, as before, as a representative test from Set 1. A comparison between Fig. 32 and Fig. 33 shows a correspondence between pressure and mass loss rate, i.e. higher pressures correspond to higher mass loss rates. The mass loss rate declines with time during all the experiments, as a result of the decreasing oxygen concentration (Fig. 34).

Pressure modeling is one of several methods used to relate reduced-scale experiments to full-scale fire behavior. The concept

has been derived and discussed extensively in the literature [4,5,6]. One of the results from the pressure modeling theory is that fuel mass flux is proportional to pressure to the two-thirds power. Figure 35 is a log-log plot of mass loss rate versus pressure at two different oxygen concentrations, 21 vol-% and 18 vol-%. These were the nominal concentrations of oxygen inside the chamber at the beginning and end of the 1 hr experiments. Note that the experimental data fall very near the two lines with slopes of two-thirds. The data at 21 vol-% correspond to data obtained by Lockwood et al. [7], denoted (L/C) on the figure. The data at 18 vol-% do not correspond to the data obtained by Lockwood et al., however, Lockwood's data appear to be somewhat scattered.

The relationship between pressure and mass loss rate can be used to determine the error in Fig. 23 due to the increase in pressure during an experiment. The resulting error is less than 0.6 kg/hr.

The temperature of the interior gas was not identical at the beginning and end of each of the four experiments plotted in Fig. 35. The maximum difference in the average chamber interior, as defined by the permanent vertical thermocouple arrays at each end of the chamber, was approximately 20°C (Fig. 36). This was shown (in Figs. 5, 6 and 22) not to be of significant magnitude to affect the mass loss rate.

Since the arrays were kept stationary at the "C" location during the Set 3 experiments, the average temperature of different horizontal cross-sections, as defined by the cross pieces of the movable array could not be calculated. Instead, an average of each horizontal cross piece was calculated for each test. The results are shown in Figs. 37 through 43, along with test M422A, which was also conducted with the arrays in the "C" location. The figures show seven horizontal levels, approximately 0.76 m (30 in.) apart, beginning 0.36 m (14 in.) from the lower deck. Again, significant stratification with respect to the interior gas temperature, occurred in all four experiments.

Normal fire test configuration in FIRE 1 includes grid-type decking on the lower and upper levels. The upper level deck, which separates the upper and lower sections of the chamber, was removed for all of the methanol pan fire tests to eliminate possible interference on gas flows within the chamber. One of the objectives of these tests was to determine flow field distribution within the chamber during a fire by taking detailed temperature measurements using the movable and fixed thermocouple arrays. Before this test series was concluded, the upper grid decking was replaced and four tests were run with the array in different locations in order to quantify the effect of the deck's presence. Figures 44 through 47 show the mass loss rate, oxygen concentration, pressure, and temperature, respectively. Comparison of these with the results from Set 1 experiments show that the decking had no significant effect on the burning rate of methanol. The effect on gas flows in

the chamber with and without the upper deck will be discussed in a forthcoming report.

CONCLUSION

Comparison of experimental results have shown how pressure and oxygen concentration affect the mass loss rate of methanol pan fires. As the oxygen concentration decreased from 21 vol-% to 13.5 vol-% throughout the experiments, the mass loss rate linearly decreased from 10 kg/hr to 6.6 kg/hr. Below 13.5 vol-% oxygen concentration, the mass loss rate rapidly declined. The fire self-extinguished when the oxygen concentration level approached 12 vol-%. An increase in initial chamber pressure from 14.7 psi to 23.9 psi (at 21 vol-% initial oxygen concentration) increased the burning rate by 34%. Experiments are planned at combinations of higher than ambient pressures and lower than ambient oxygen concentrations in order to quantify the combined effect of these variables on the mass loss rate of methanol. Experiments are also planned to determine the effect of pressure and oxygen concentration on the burning rates of other fuels.

REFERENCES

1. J.I. Alexander, H.J. St. Aubin, J.P. Stone, and F.W. Williams, "Large-Scale Pressurizable Fire Test Facility - Fire I," NRL Report 8643, Dec. 1982.

2. V. Babrauskas, "Burning Rates," The SFPE Handbook of Fire Protection Engineering, National Fire Protection Association, Quincy, MA (1988).

3. P.A. Tatem, "Theoretical and Experimental Investigation of Methanol Combustion under Constant Volume," Ph.D. dissertation, Department of Chemistry, George Washington University, 1984.

4. J. De Ris, A. Murty Kanury, and M.C. Yuen, "Pressure Modeling of Fires," Fourteenth Symposium (International) on Combustion, The Combustion Institute (1973), p. 1033.

5. J.G. Quintiere, "Scaling Applications in Fire Research," Fire Safety Journal 15:1 (1989).

6. R.L. Alpert, "Pressure Modeling of Transient Crib Fires," FMRC Serial 22360-2, Factory Mutual Research Corp, Norwood, MA (1975).

7. R.W. Lockwood and R.C. Corlett, "Radiative and Convective Feedback Heat Flux in Small Turbulent Pool Fires with Variable Pressure and Ambient Oxygen," Proceedings of the 1987 ASME:JSME Thermal Engineering Joint Conference, Honolulu, HA (1987).

Table 1 - Methanol Pan Fires Varying Initial Oxygen Concentrations and Chamber Pressure

TEST	MOVABLE THERMOCOUPLE ARRAY LOCATION	INITIAL OXYGEN CONC (VOL-%)	INITIAL PRESSURE (PSI)
Set 1:			
M418A	TOP: OVER FUEL PAN BTM: C	21	14.7
M419A	C	21	14.7
M422A	C	21	14.7
M423A	BETWEEN B AND C	21	14.7
M423B	BETWEEN B AND C	21	14.7
M424A	B	21	14.7
M424B	B	21	14.7
M425A	BETWEEN A AND B	21	14.7
Set 2:			
M425B	B	17	14.7
M430A	BETWEEN B AND C	15	14.7
M430B	C	15	14.7
Set 3:			
M502A	C	21	23.9
M503A	C	21	17.6
M514A	C	21	20.7
Set 4:			
M617A	BETWEEN A AND B	21	14.7
M618A	B	21	14.7
M619A	BETWEEN B AND C	21	14.7
M619B	C	21	14.7

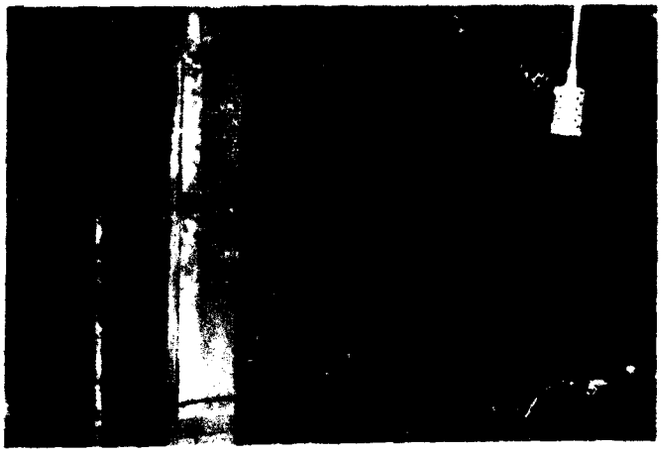

Figure 1 - First thermocouple array

Figure 2 - Thermocouple array, by deck

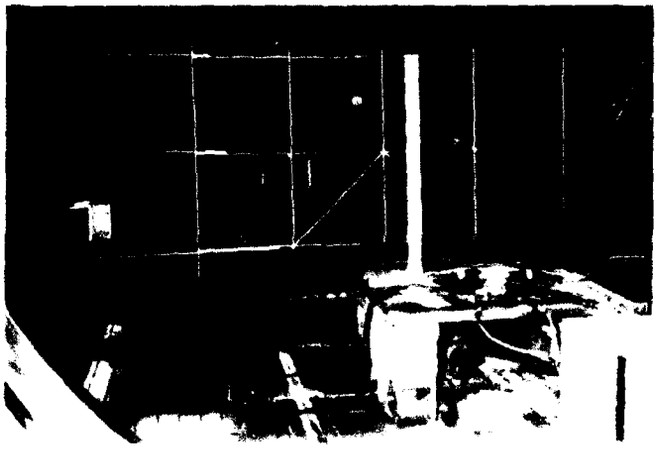

Figure 3 - Thermocouple array, lower deck. Pictured in the foreground is the fuel supply system and fire pan

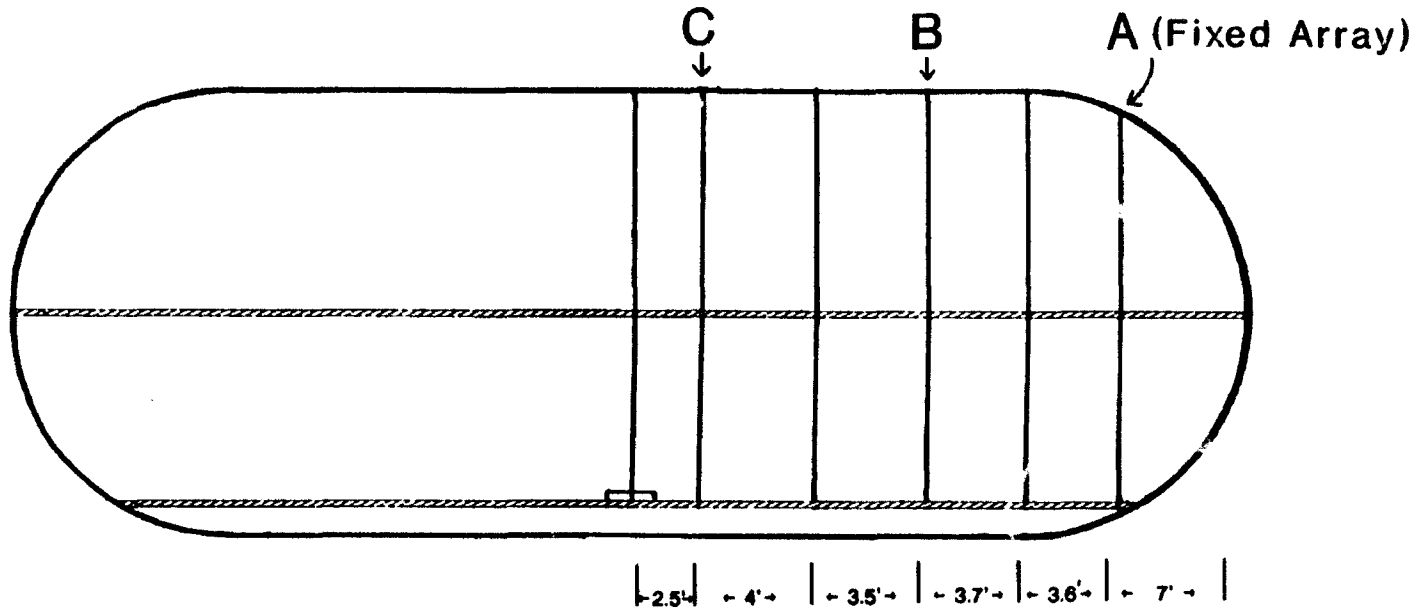

Figure 4. Thermocouple Array Locations.

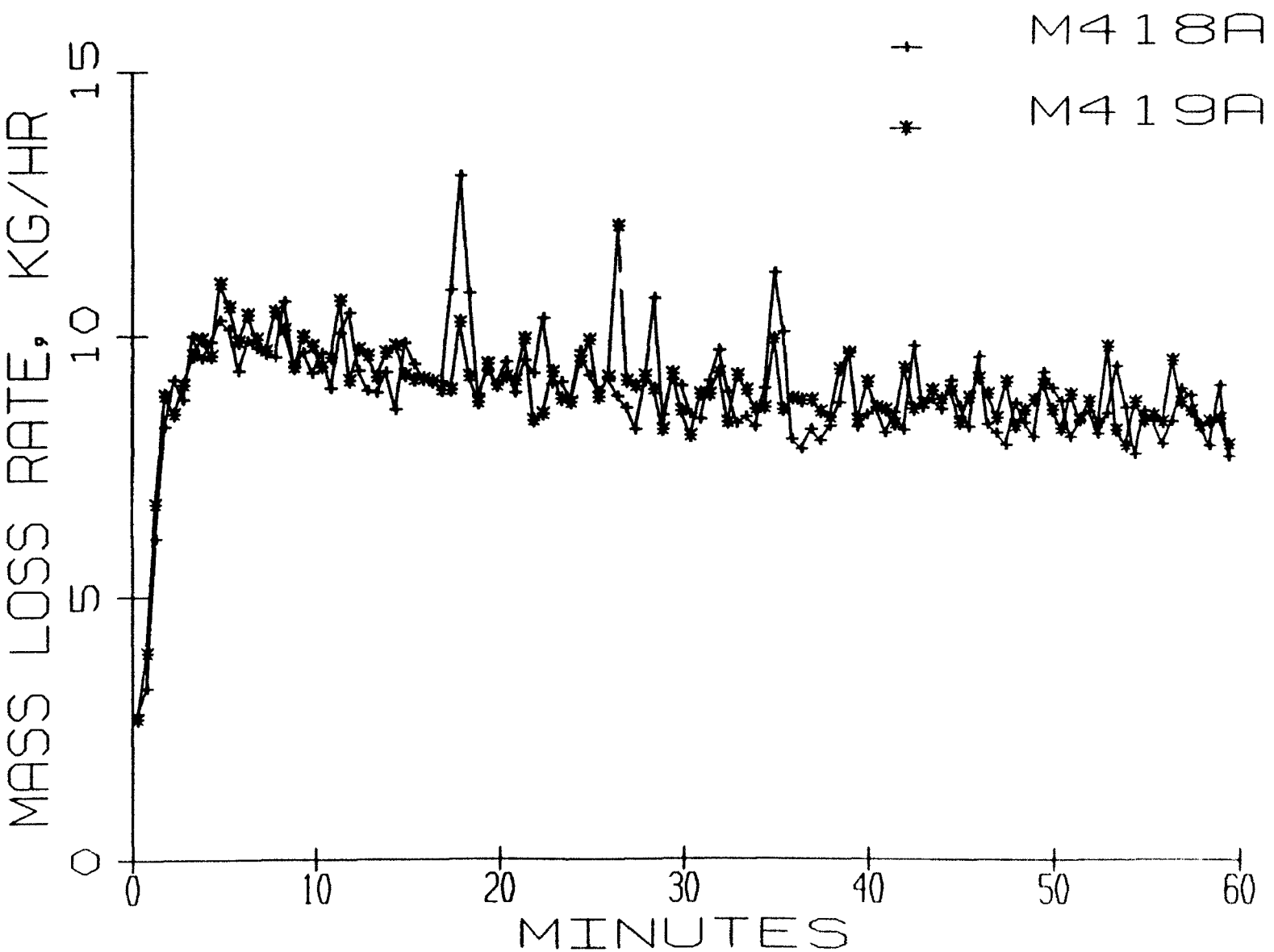

Fig. 5 - Mass loss rate of fuel

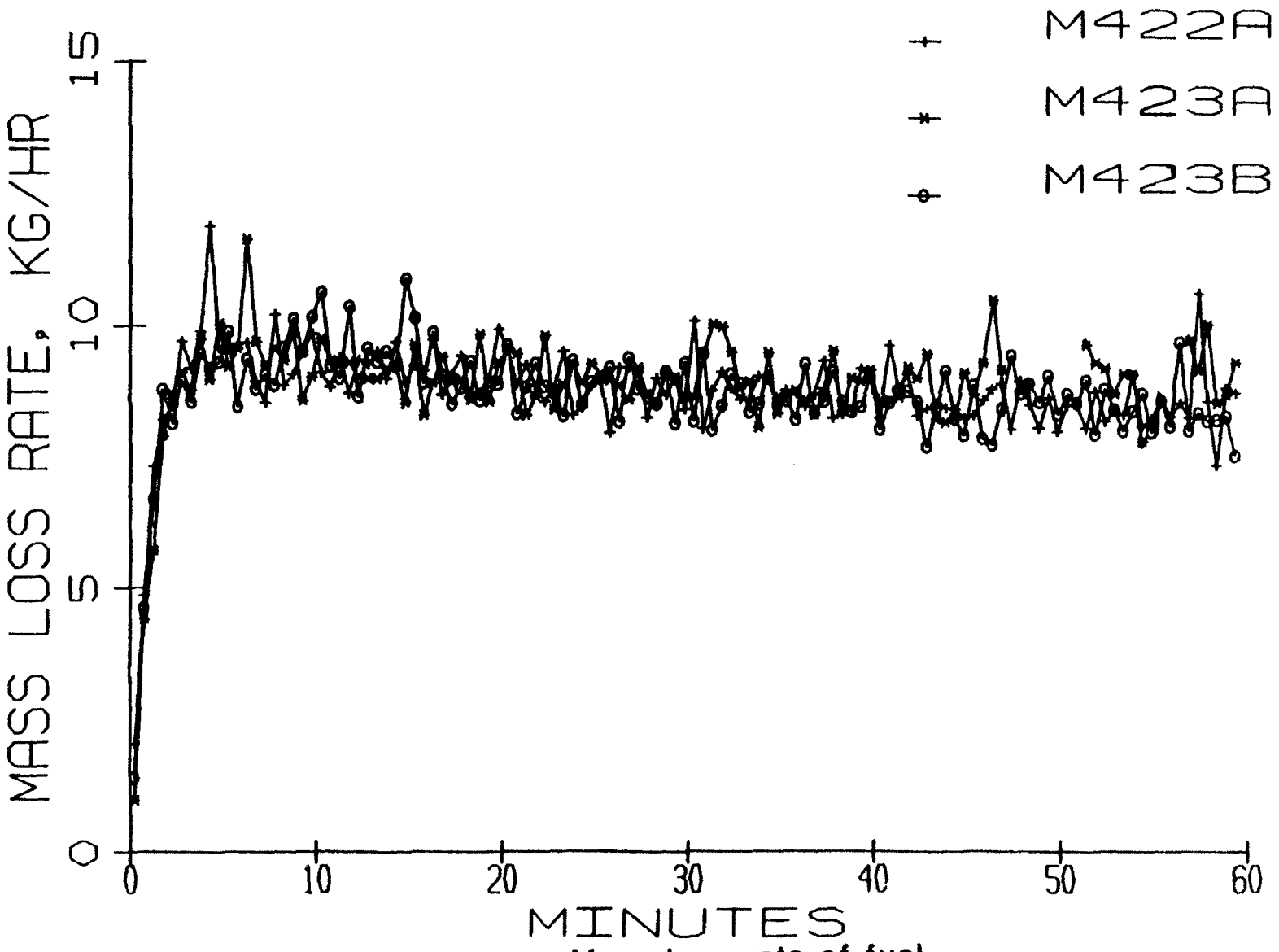

Fig. 6 - Mass loss rate of fuel

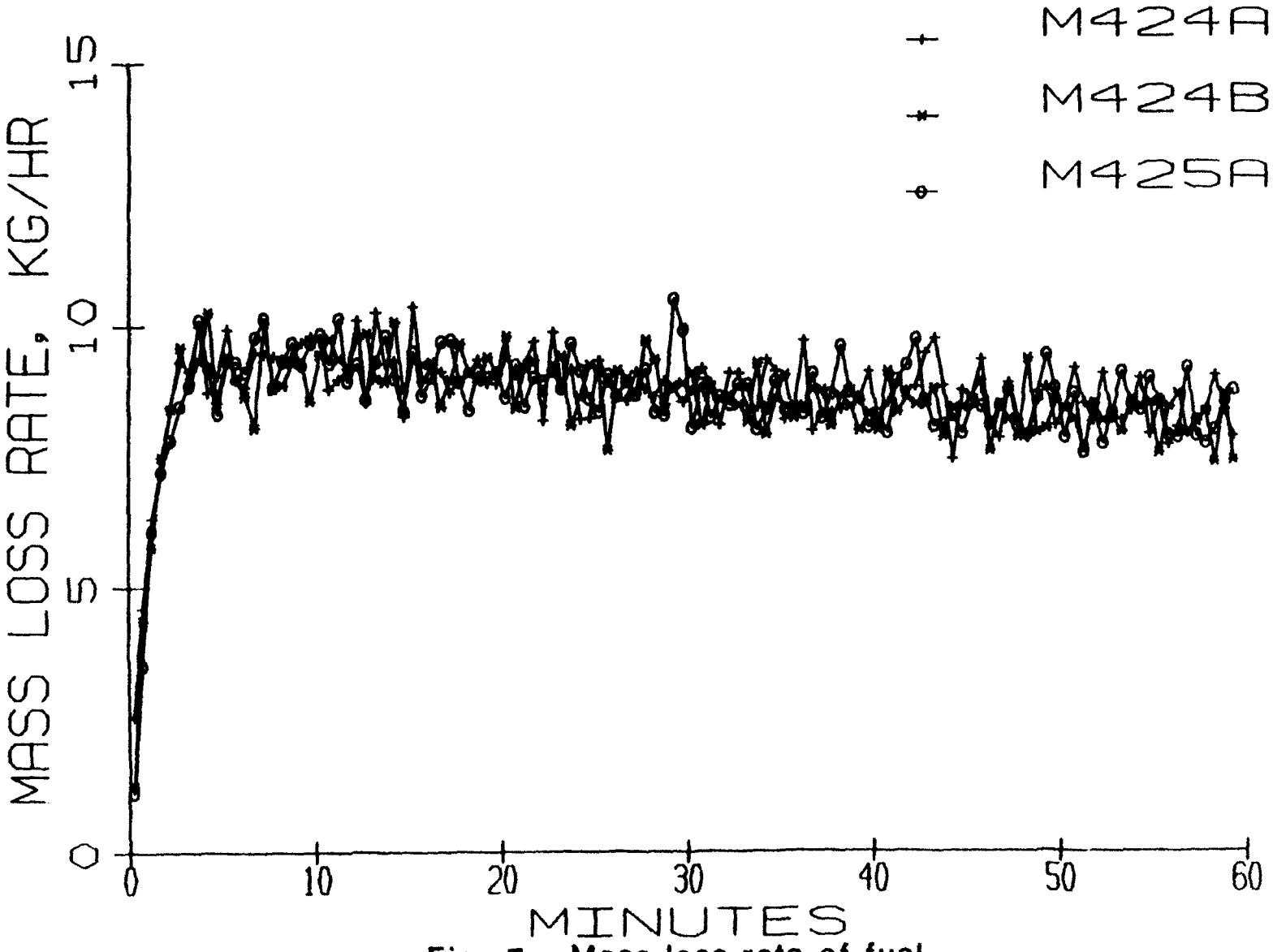

Fig. 7 - Mass loss rate of fuel

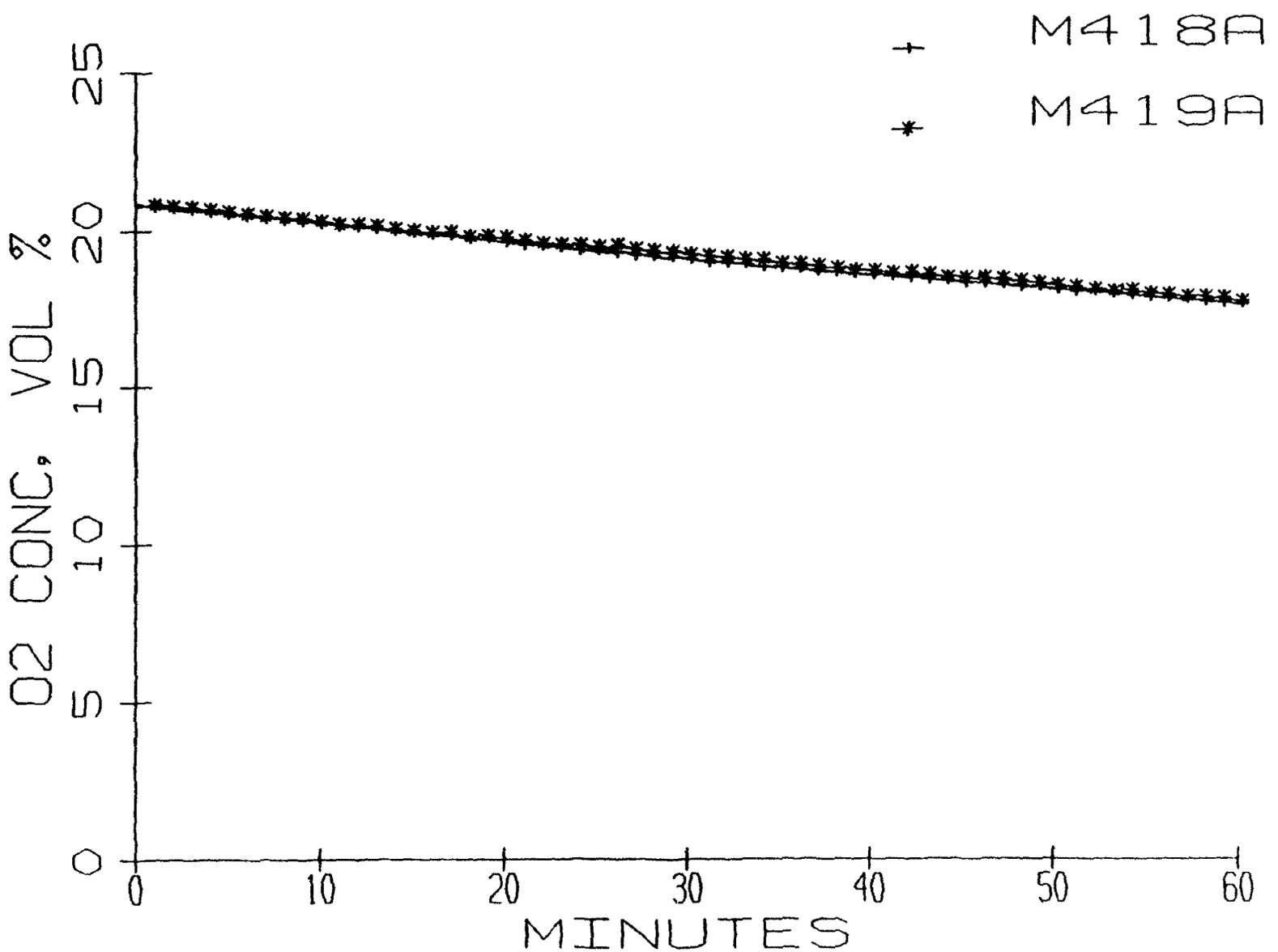

Fig. 8 - Average oxygen concentration

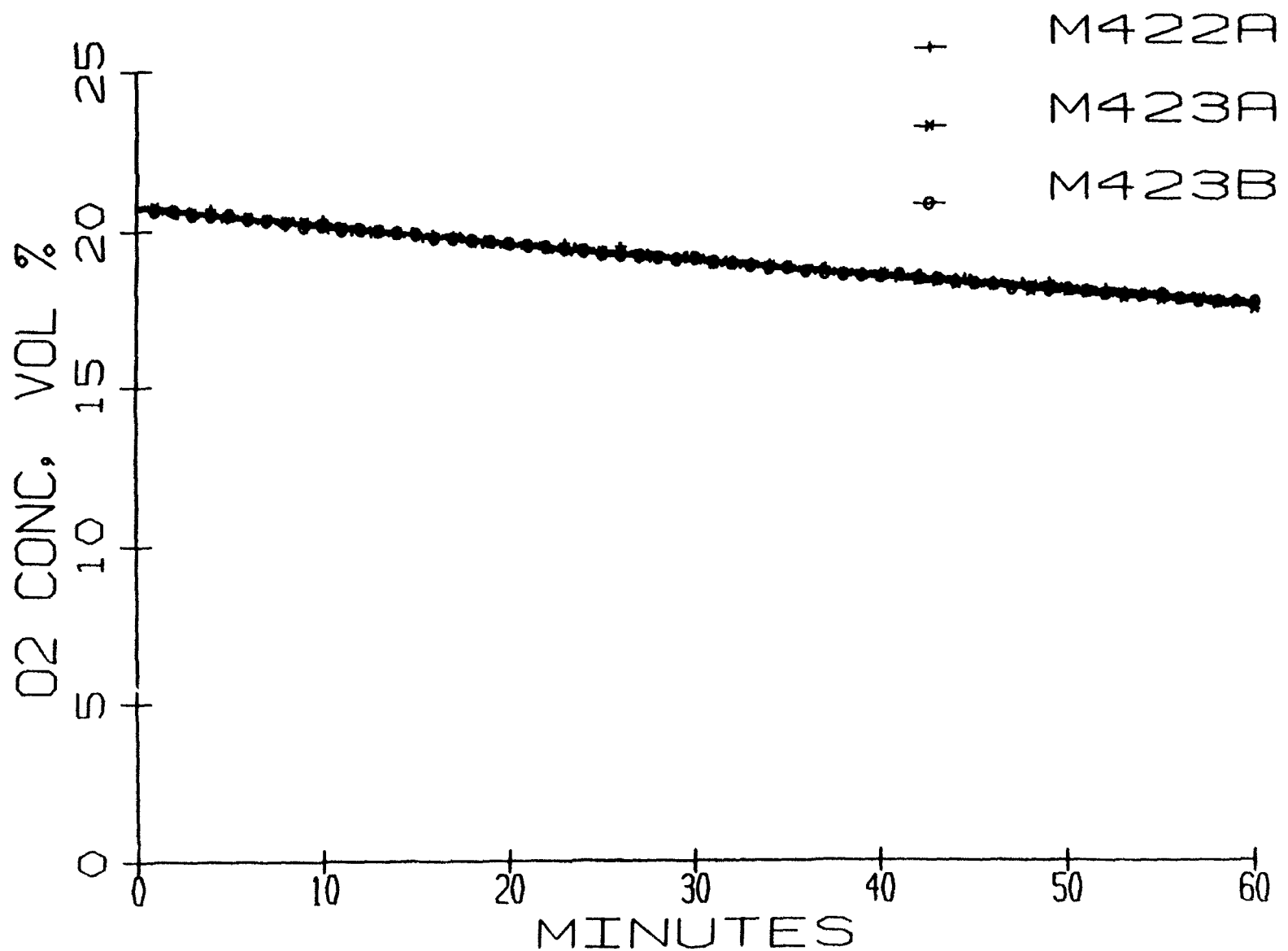

Fig. 9 - Average oxygen concentration

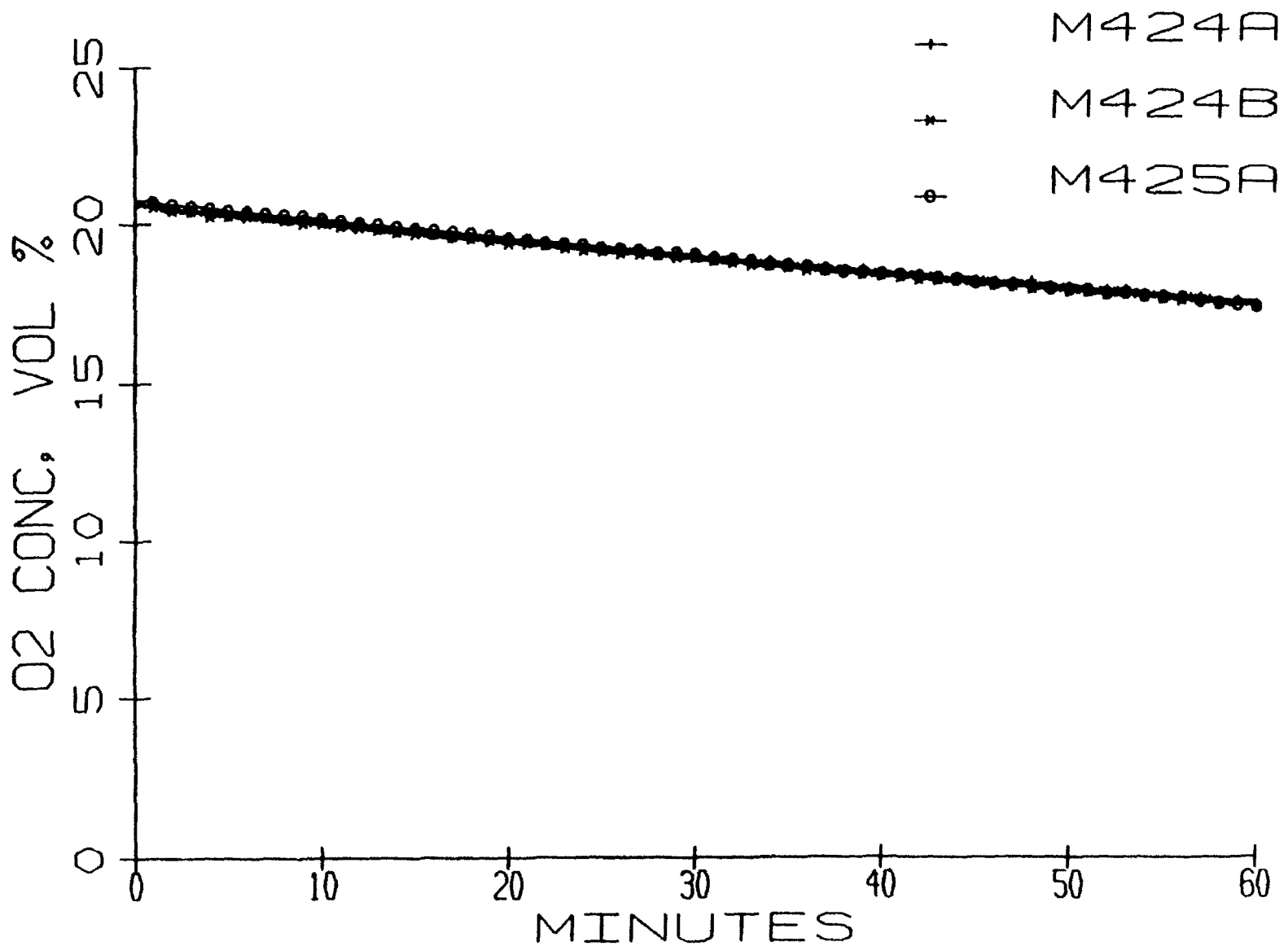

Fig. 10 - Average oxygen concentration

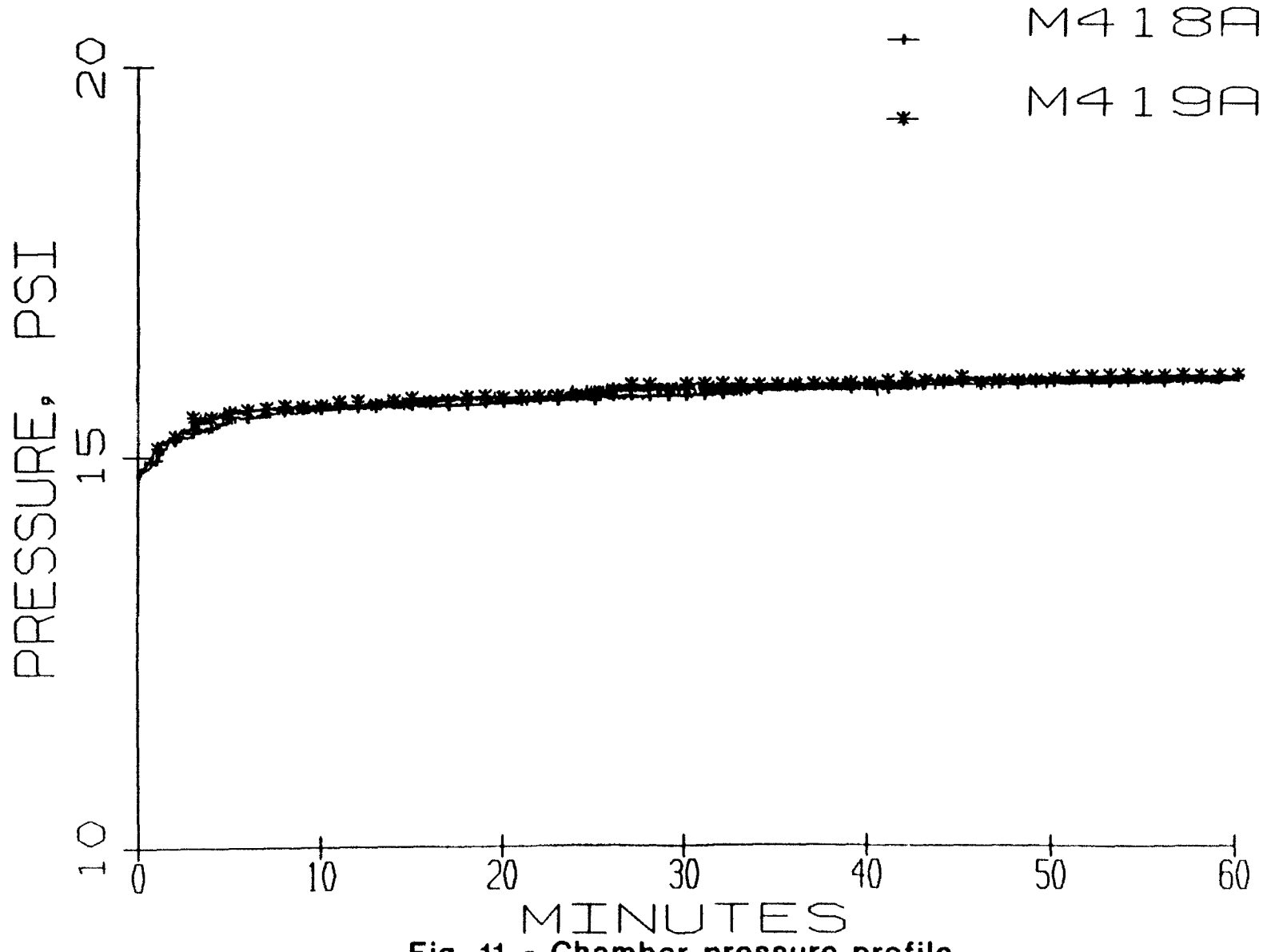

Fig. 11 - Chamber pressure profile

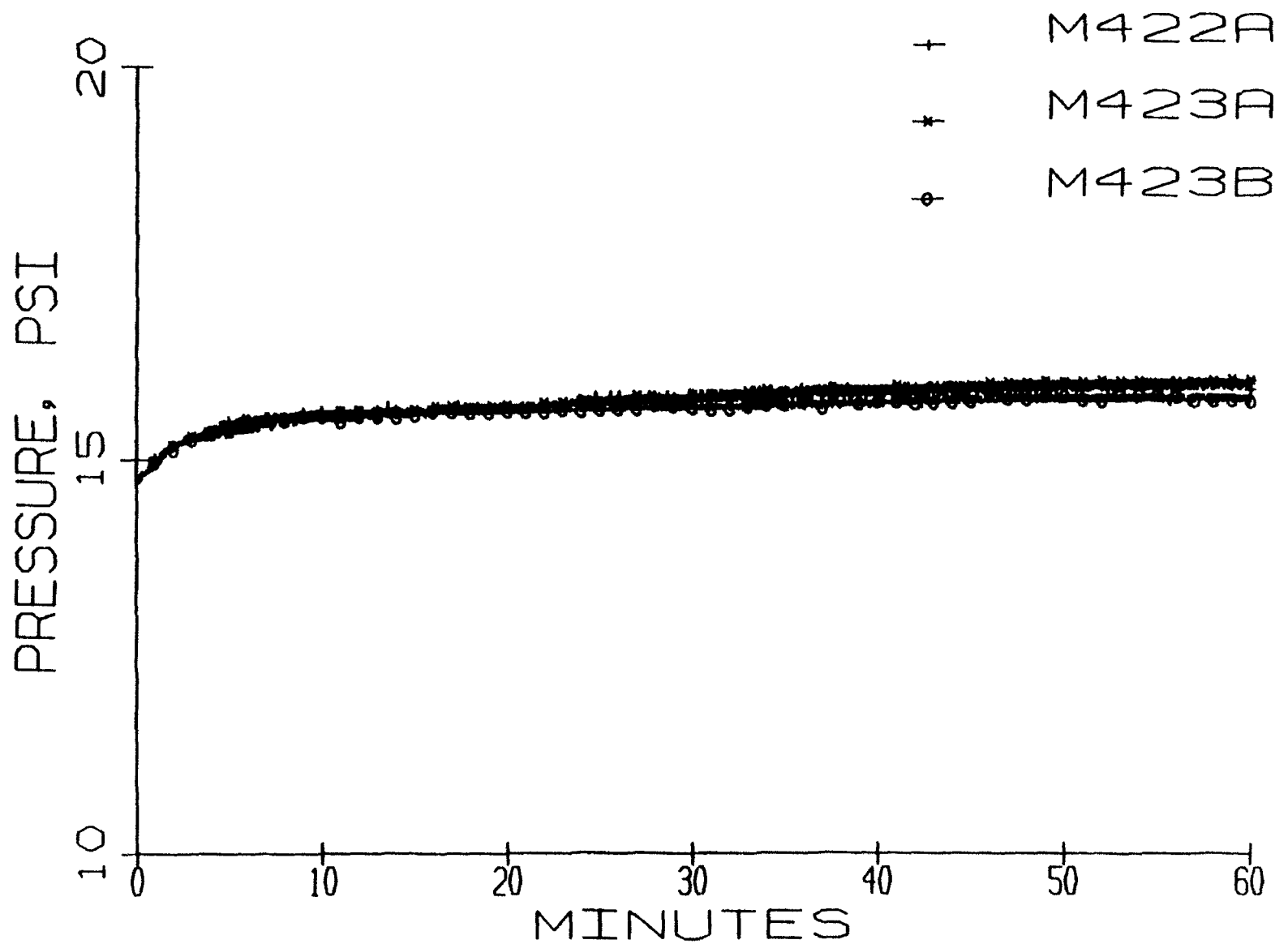

Fig. 12 - Chamber pressure profile

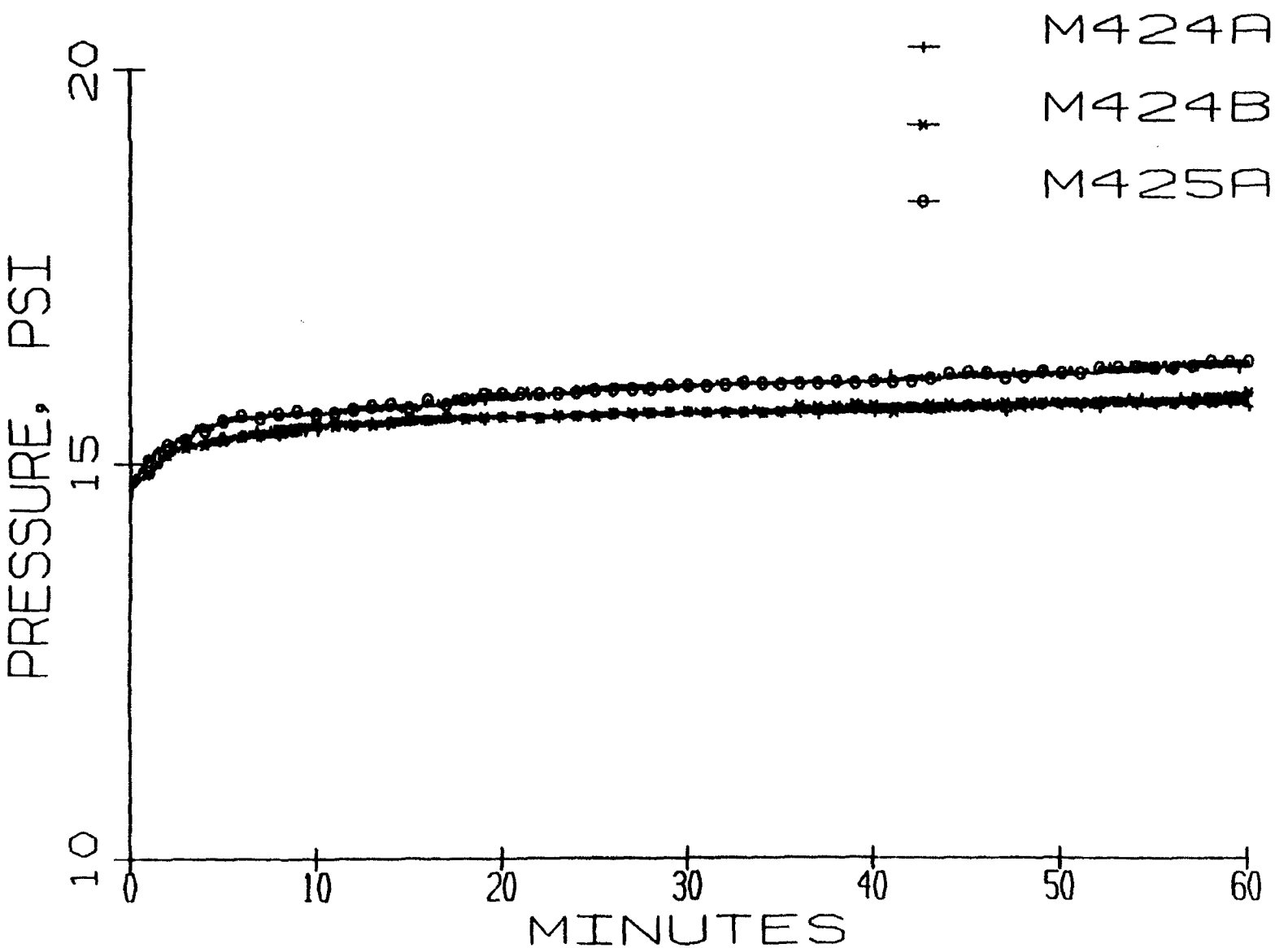

Fig. 13 - Chamber pressure profile

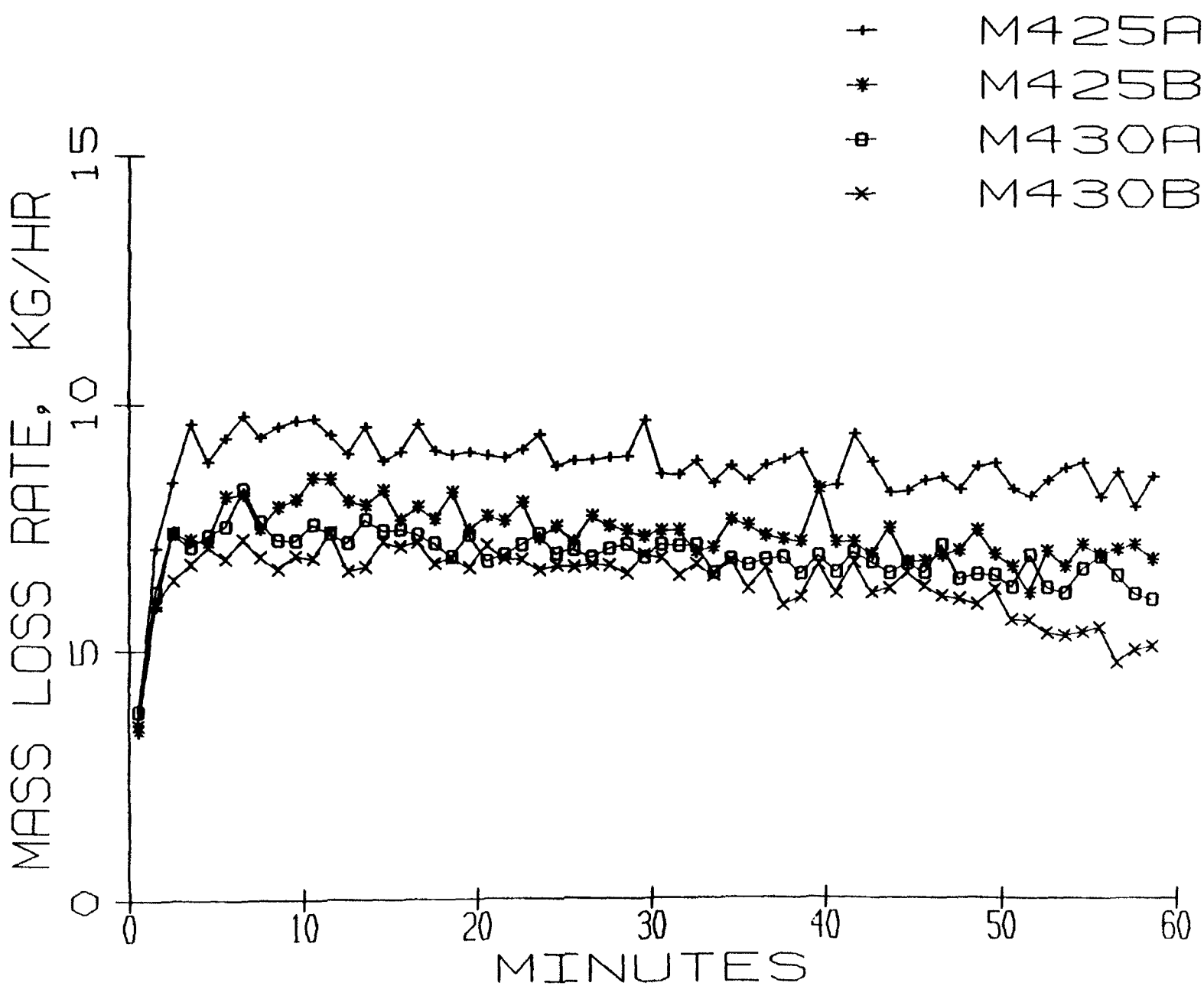

Fig. 14 - Mass loss rate of fuel at different initial O2 concentrations

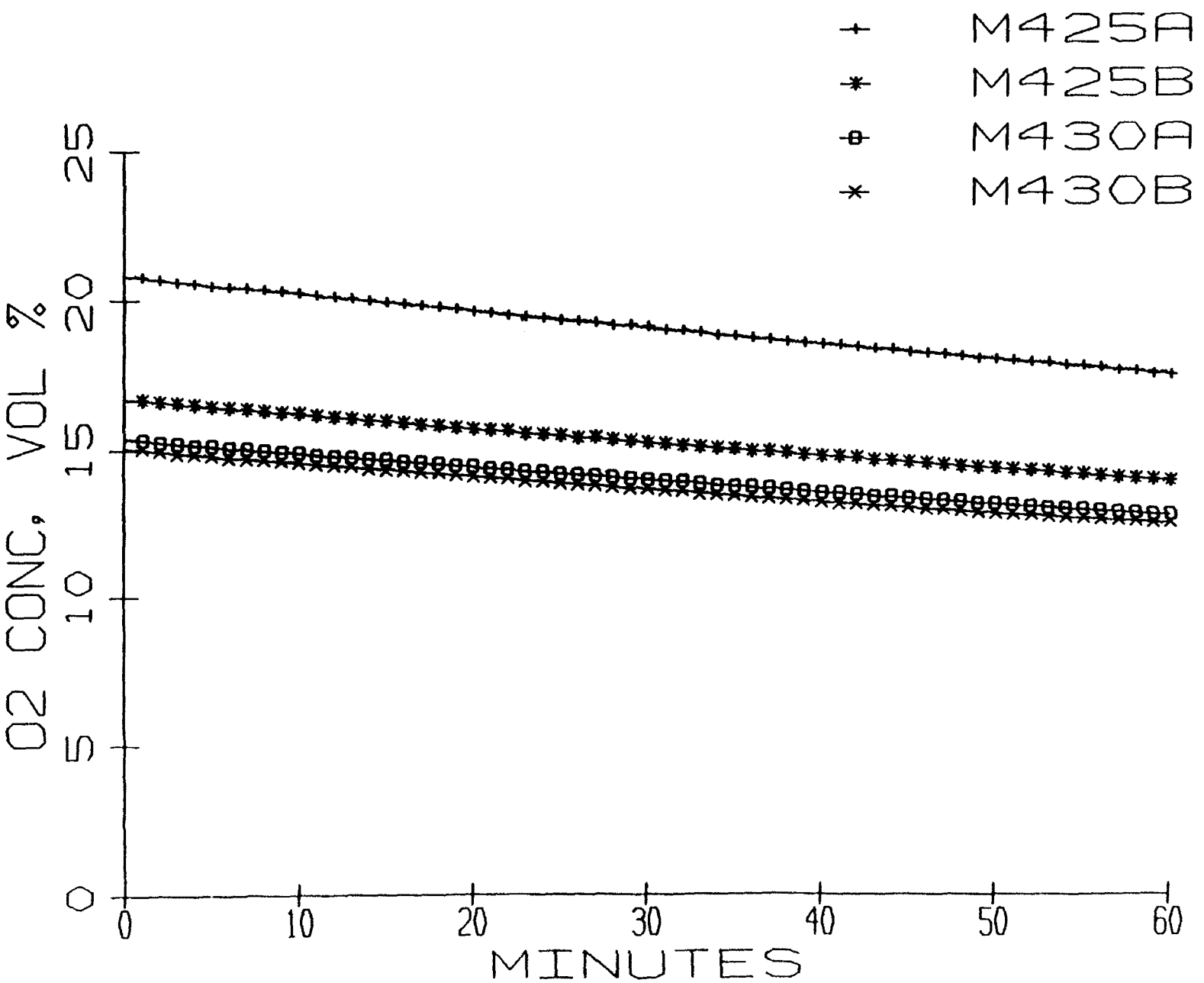

Fig. 15 - Average oxygen concentration

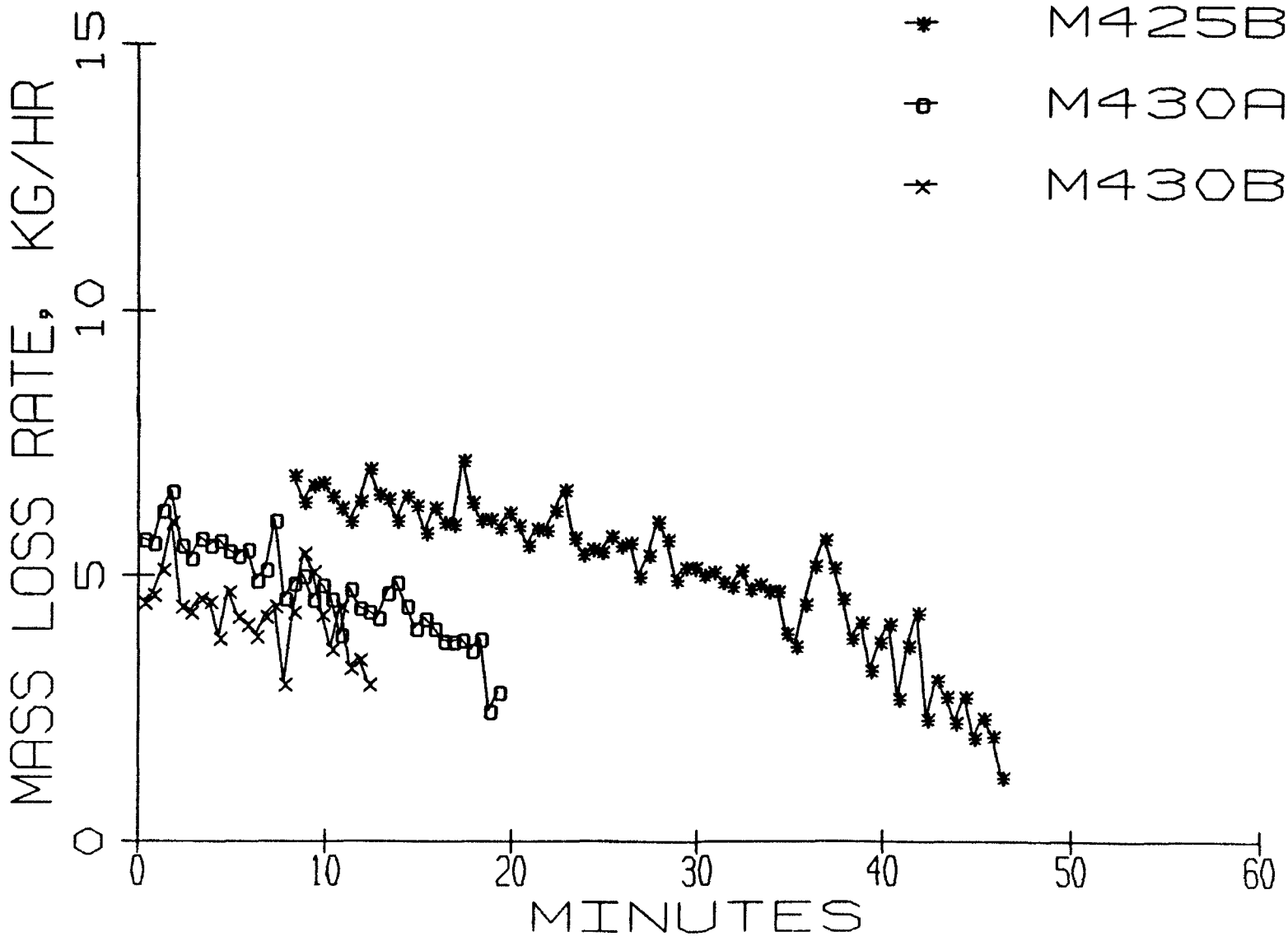

Fig. 16 - Mass loss rate of fuel after one hour burn time until self-extinguishment

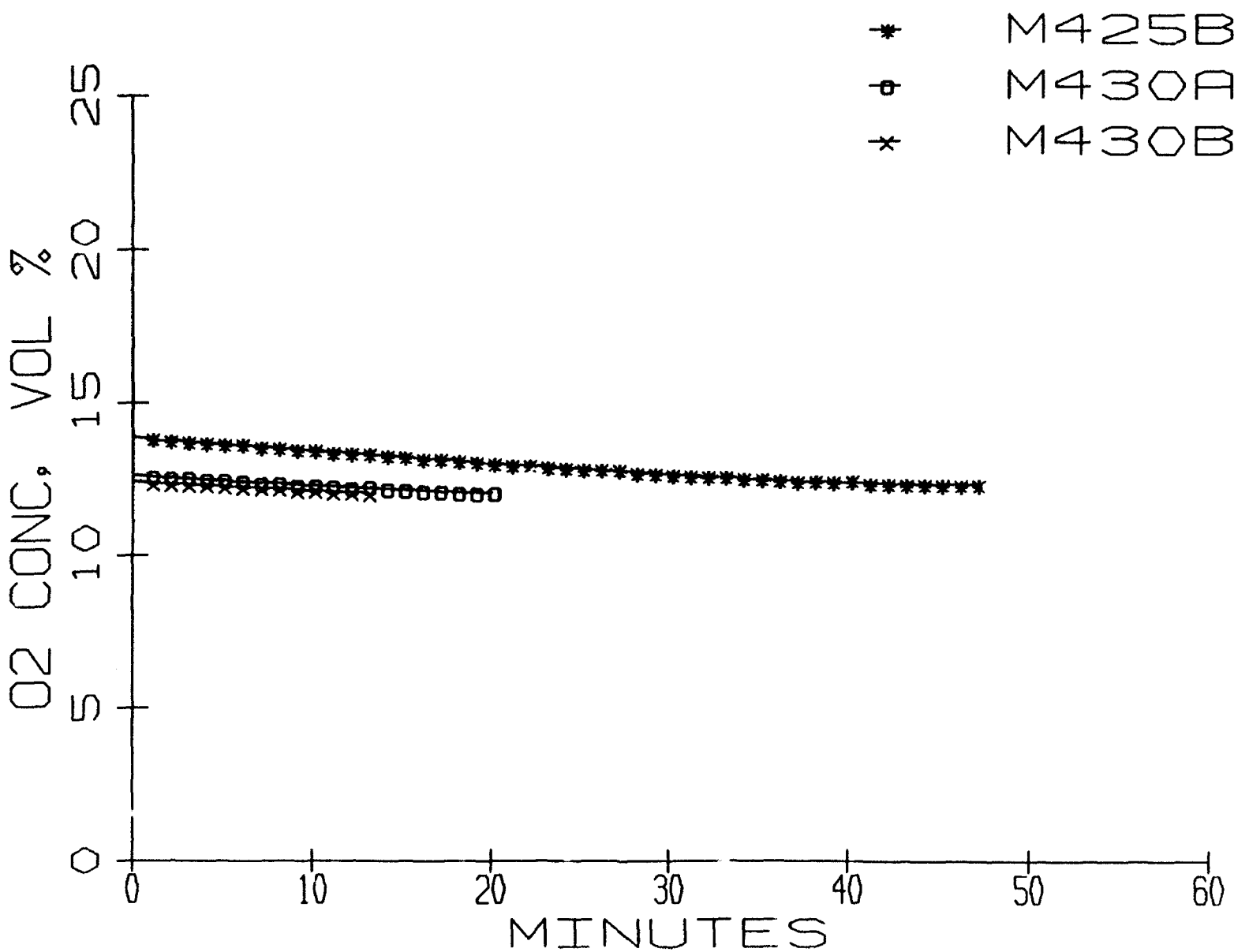

Fig. 17 - Oxygen conc. after one hour burn time until self-extinguishment

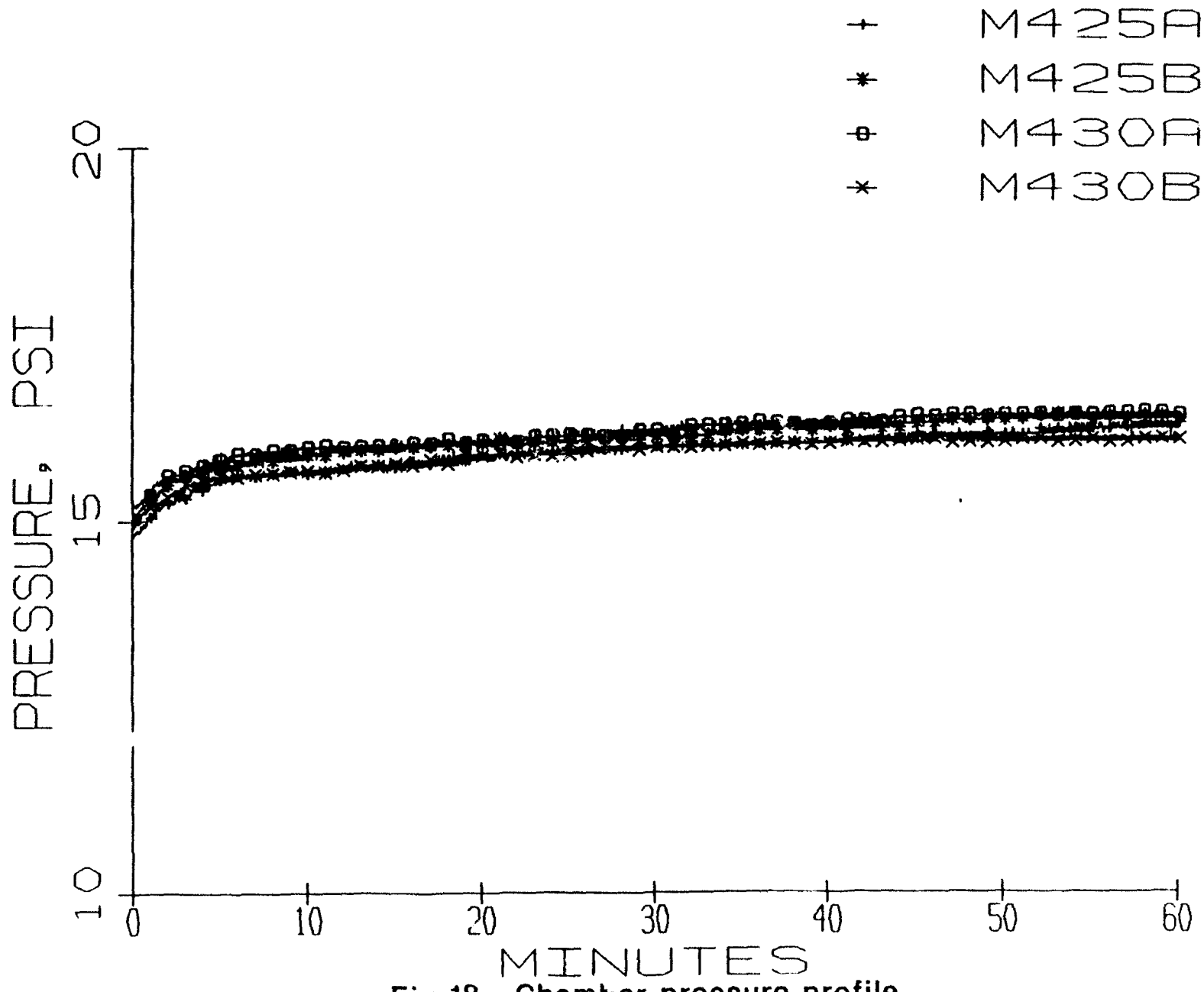

Fig. 18 - Chamber pressure profile

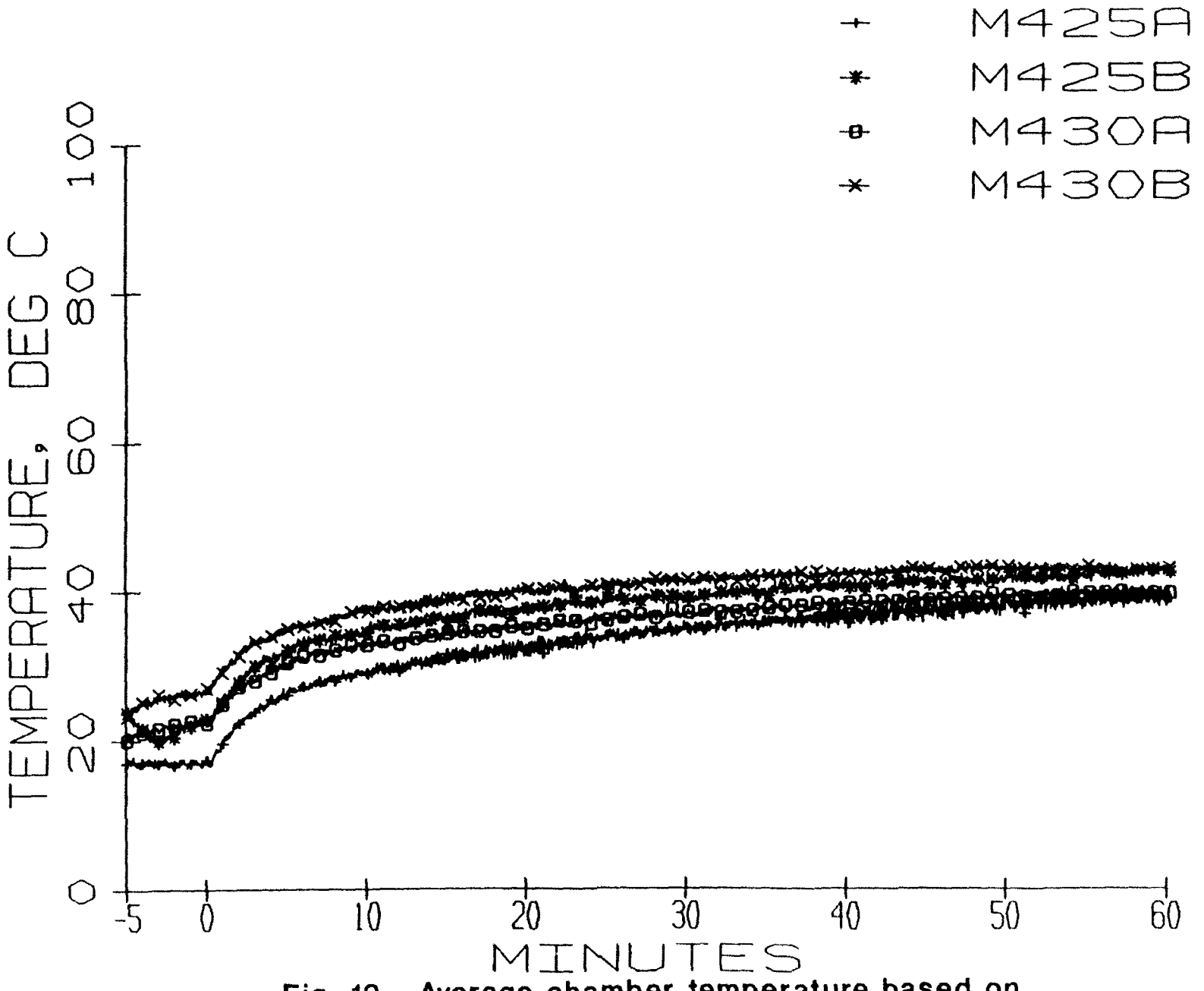

Fig. 19 - Average chamber temperature based on fwd and aft thermocouple trees

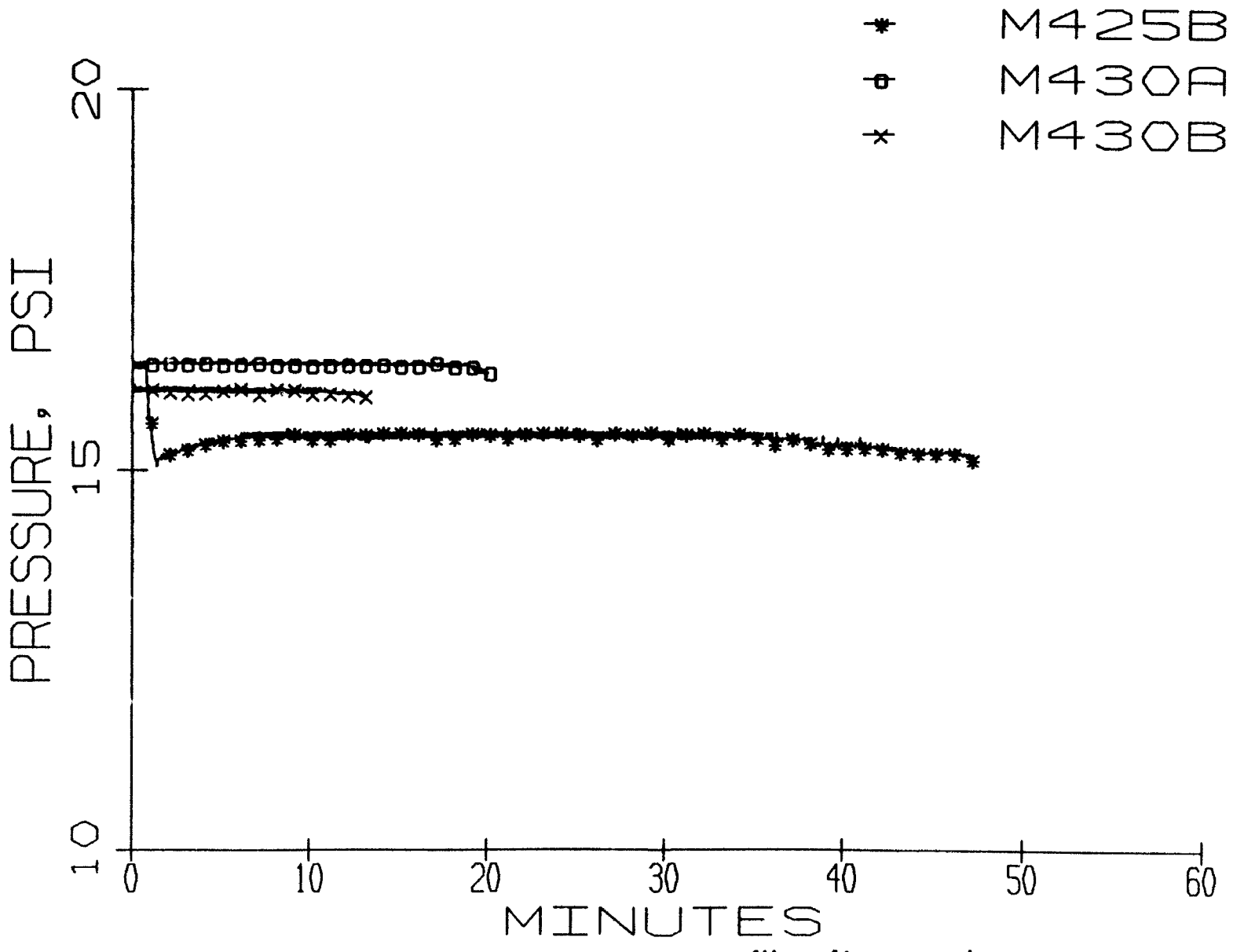

Fig. 20 - Chamber pressure profile after one hour burn time until self-extinguishment

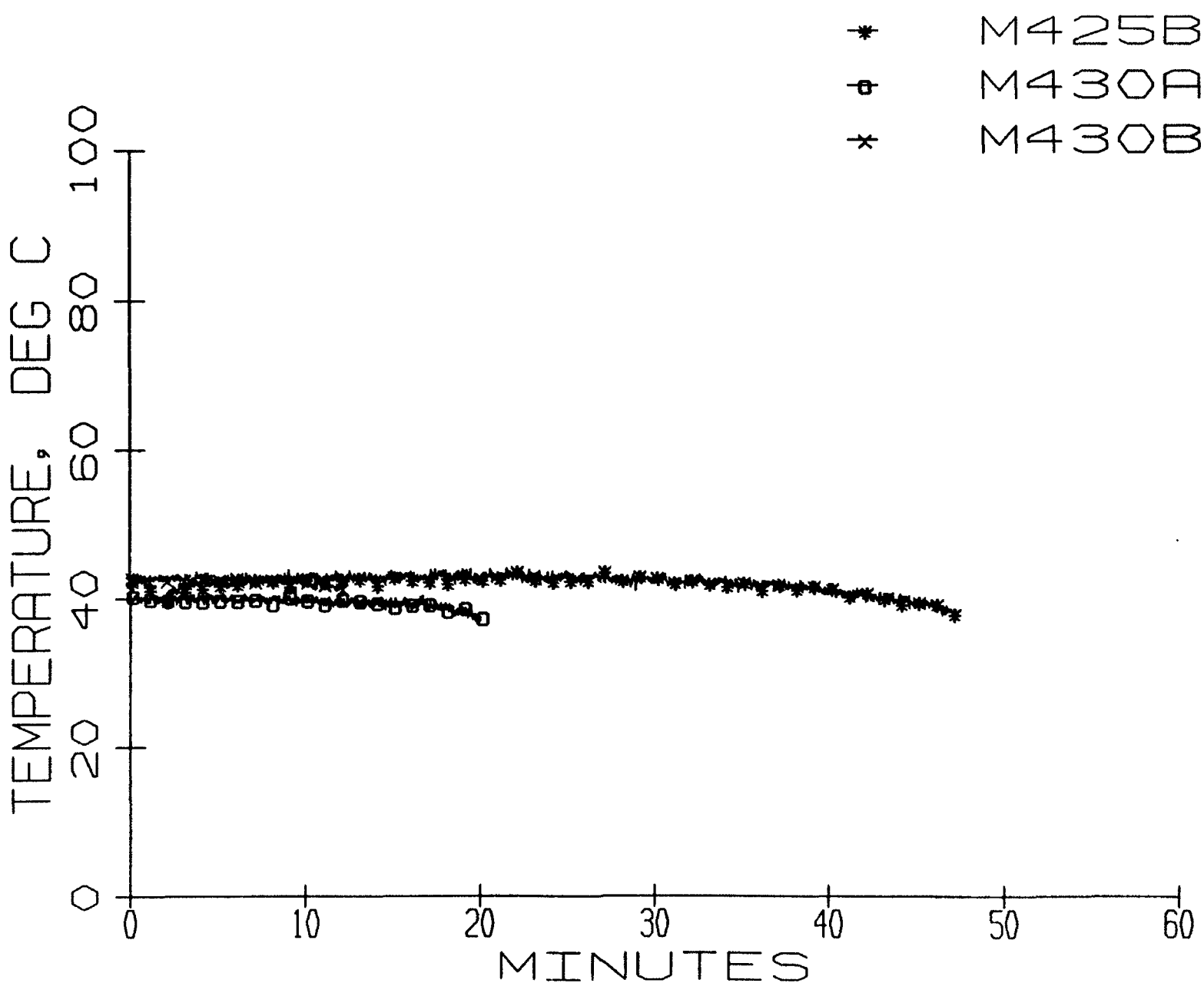

Fig. 21 - Average chamber temperature after one hour burn time until self-extinguishment

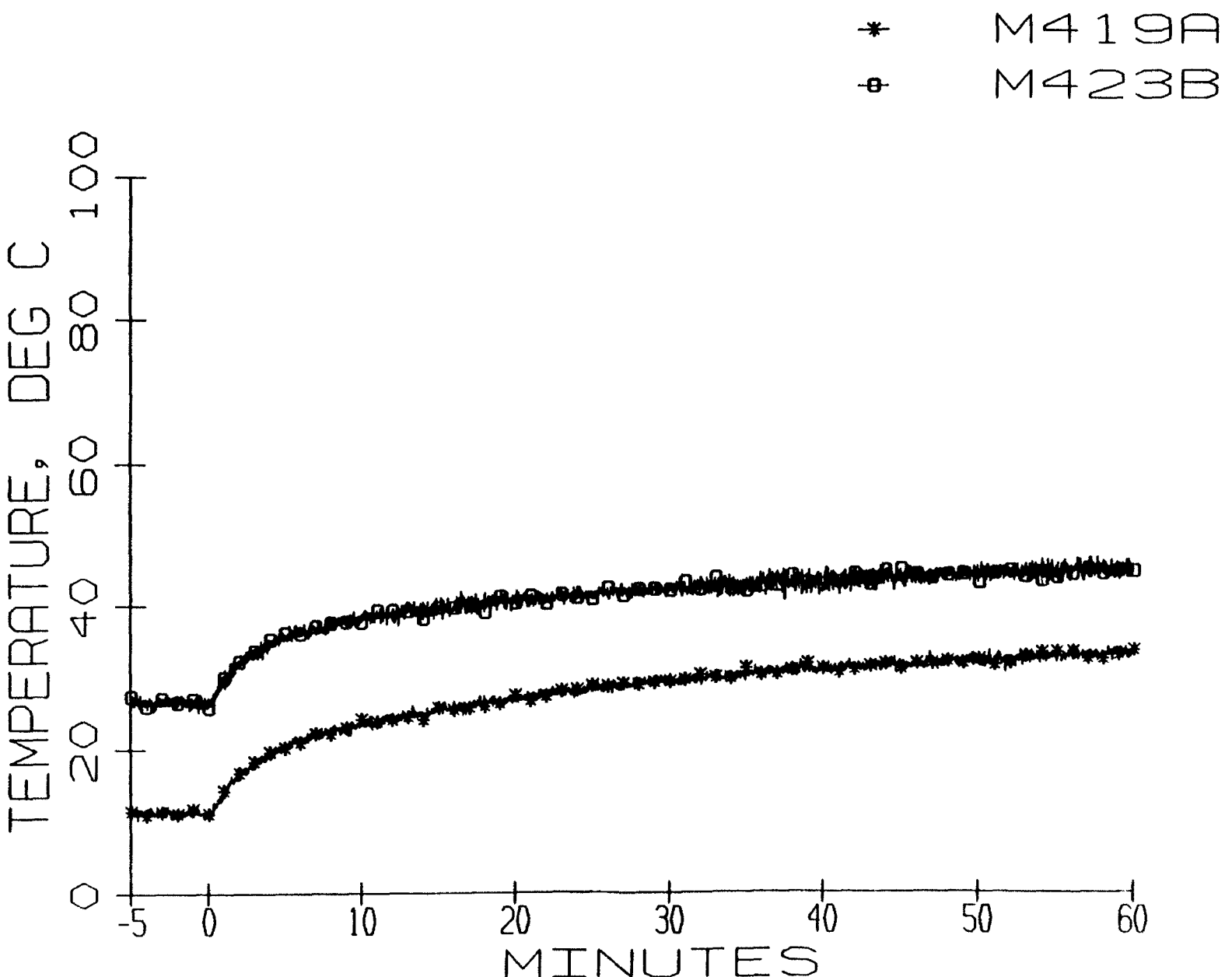

Fig. 22 - Average chamber temperature based on fwd and aft thermocouple trees

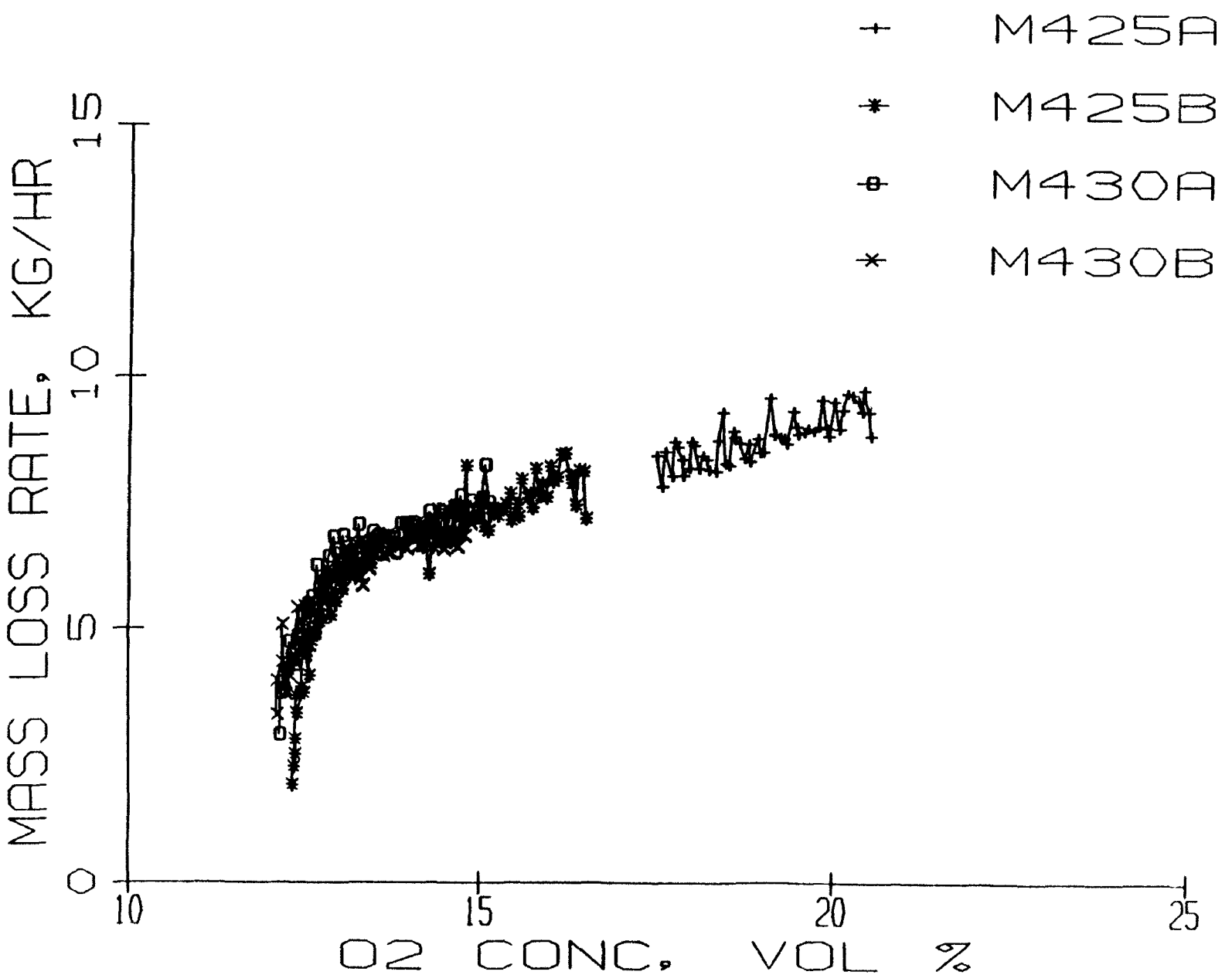

Fig. 23 - Mass loss rate of fuel as a function of oxygen concentration

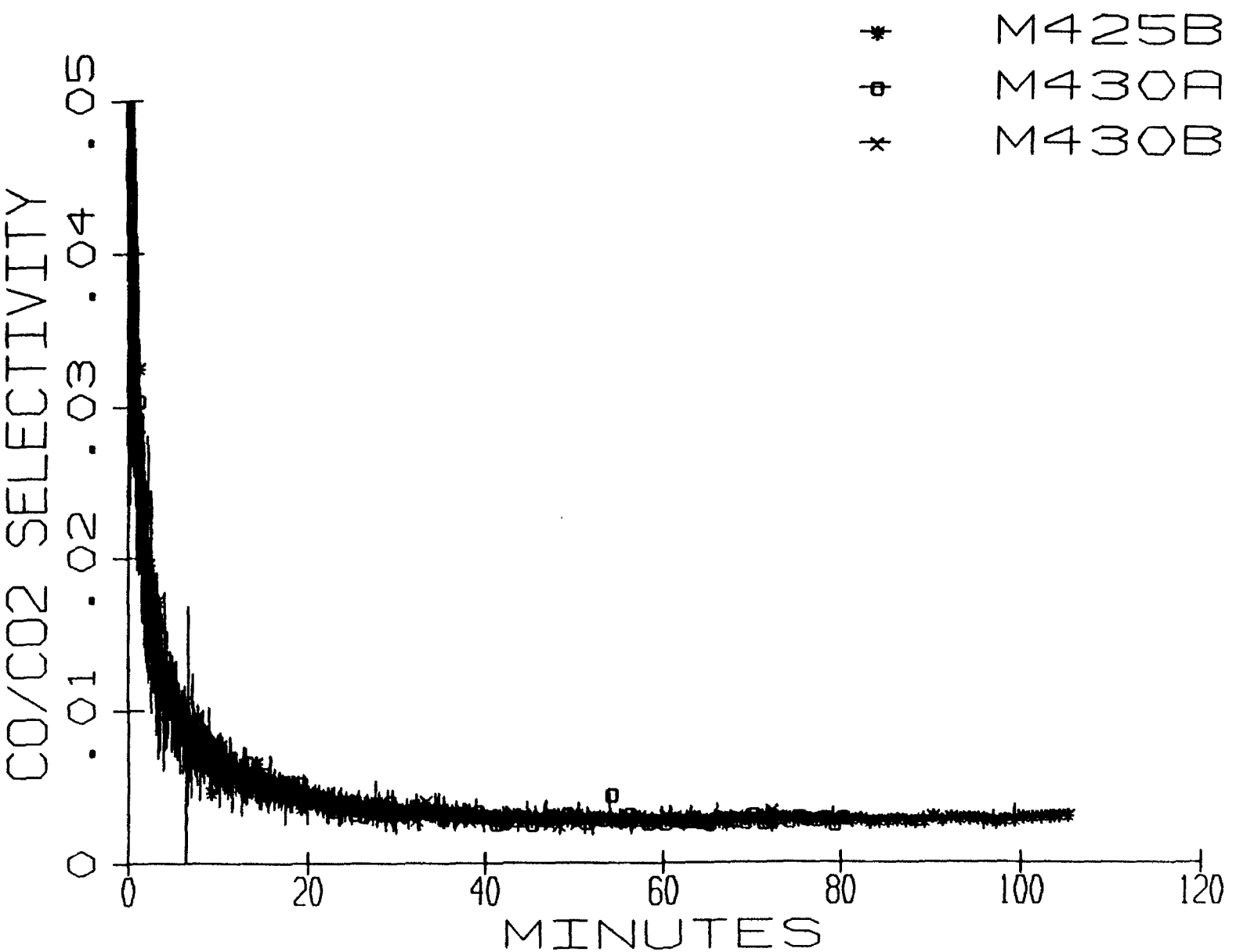

Fig. 24 - CO/CO2 mole ratio

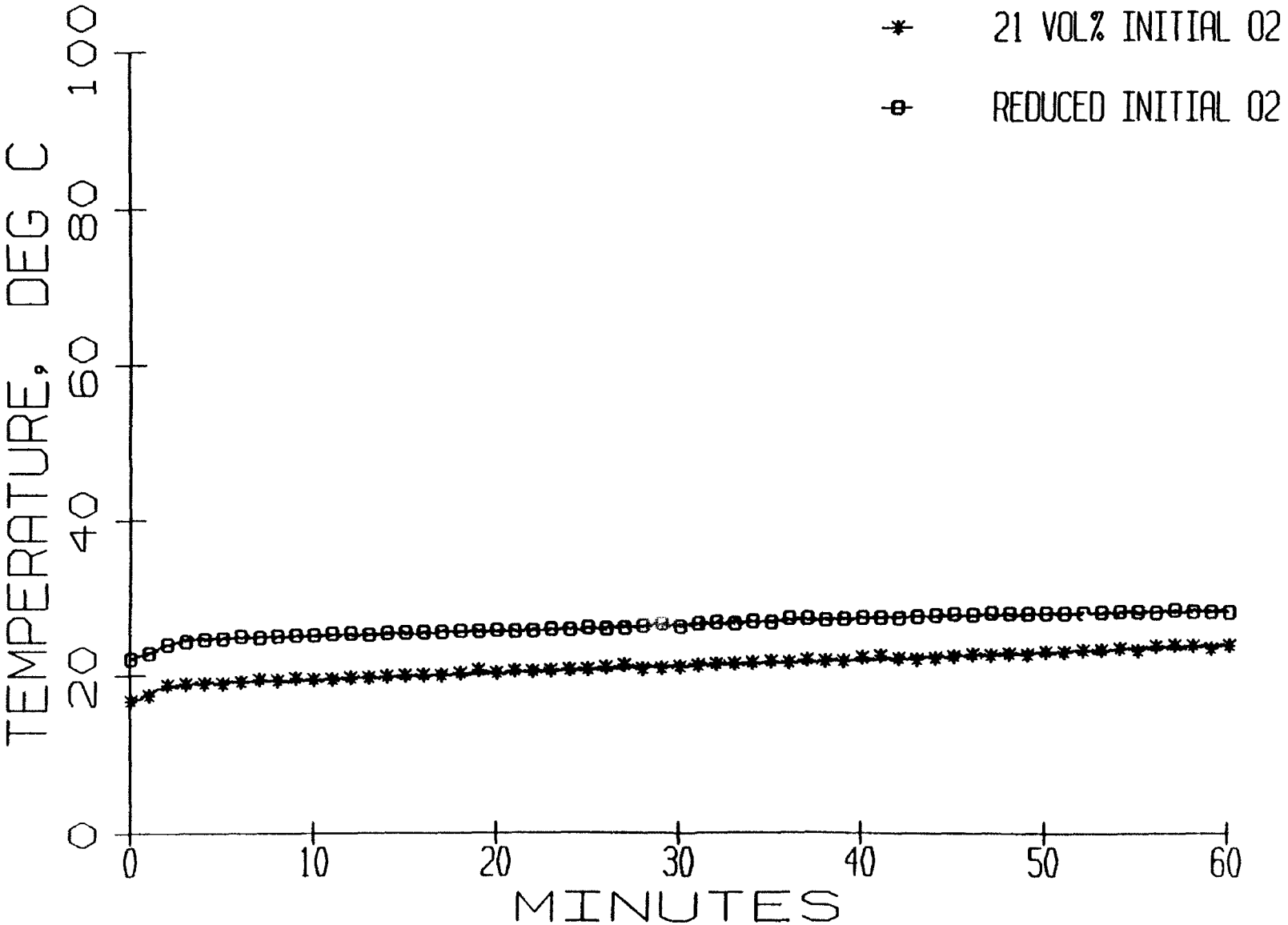

Fig. 25 - Average temperature profile of horizontal cross section approximately 0.36 m (14 in.) from lower deck

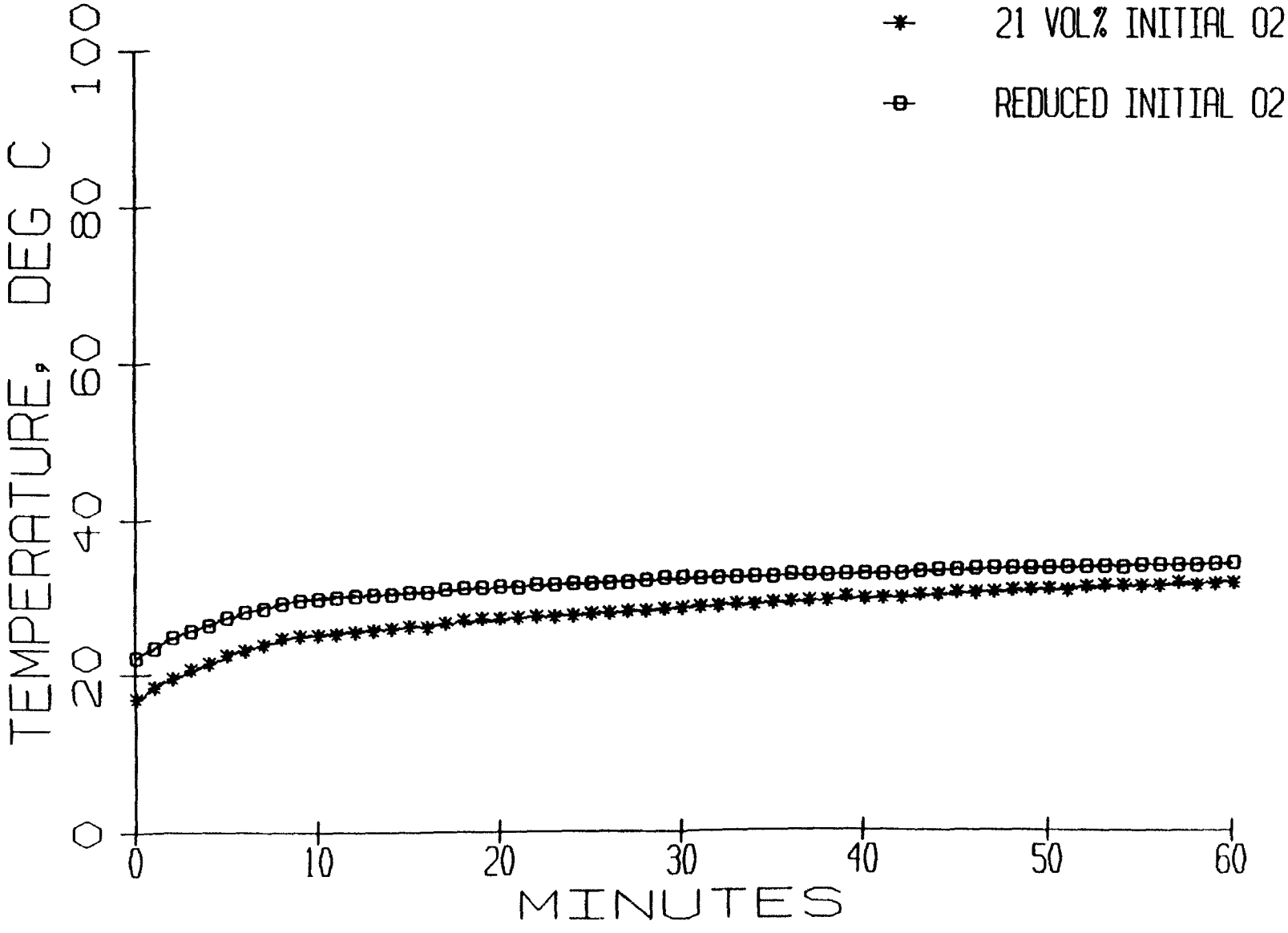

Fig. 26 - Average temperature profile of horizontal cross section approximately 1.12 m (44 in.) from lower deck

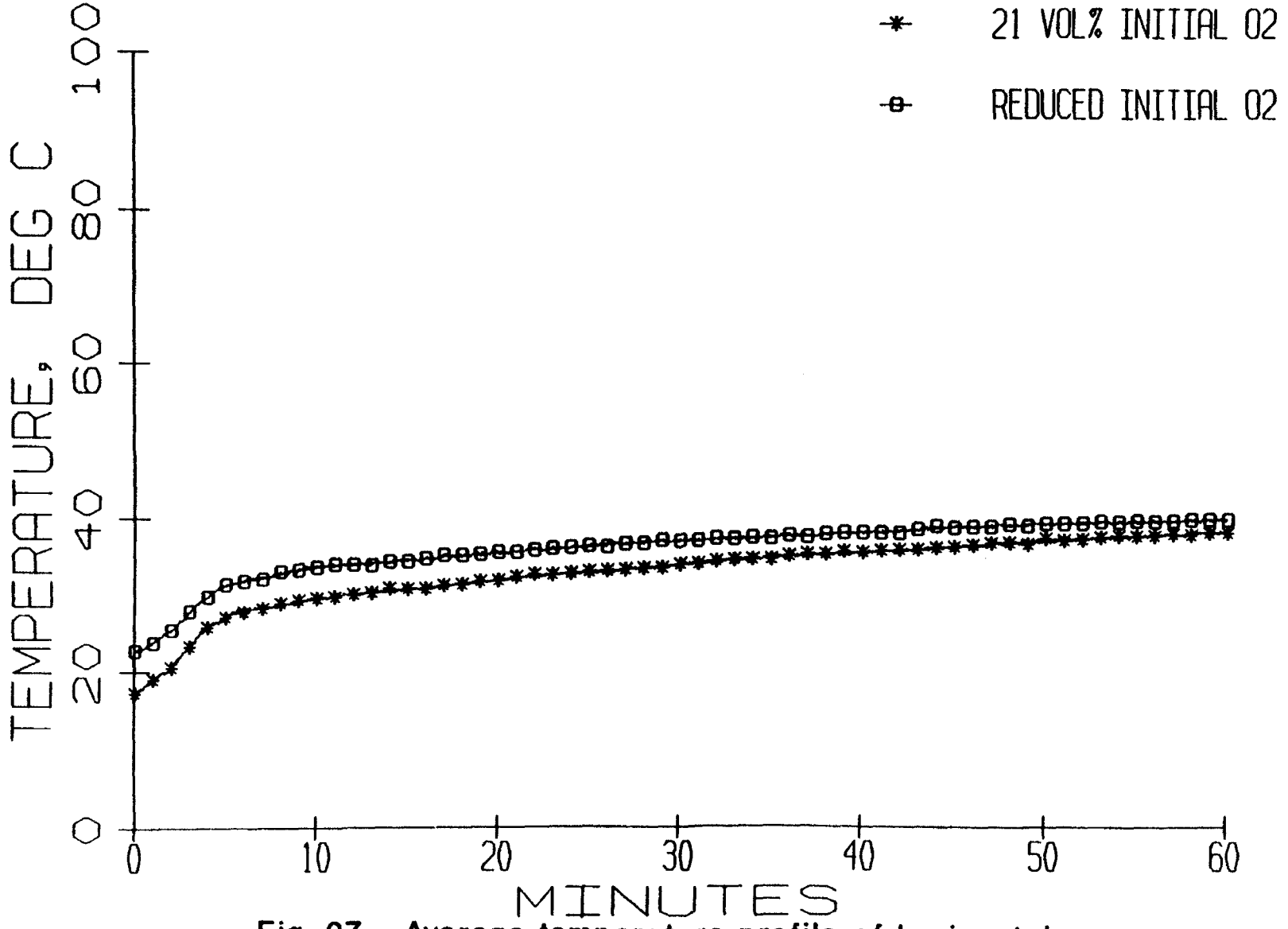

Fig. 27 - Average temperature profile of horizontal cross section approximately 1.88 m (74 in.) from lower deck

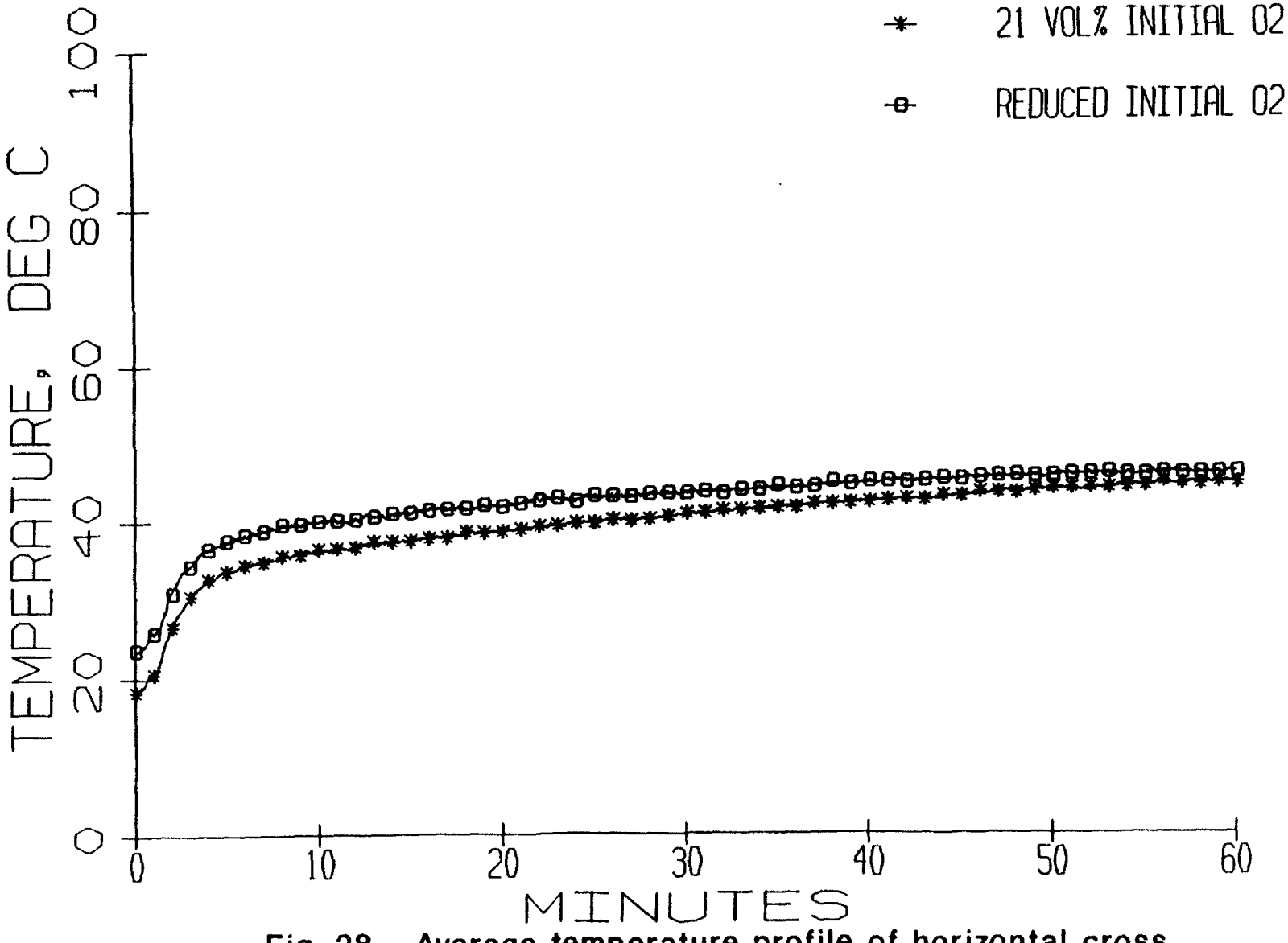

Fig. 28 - Average temperature profile of horizontal cross section approximately 2.64 m (104 in.) from lower deck

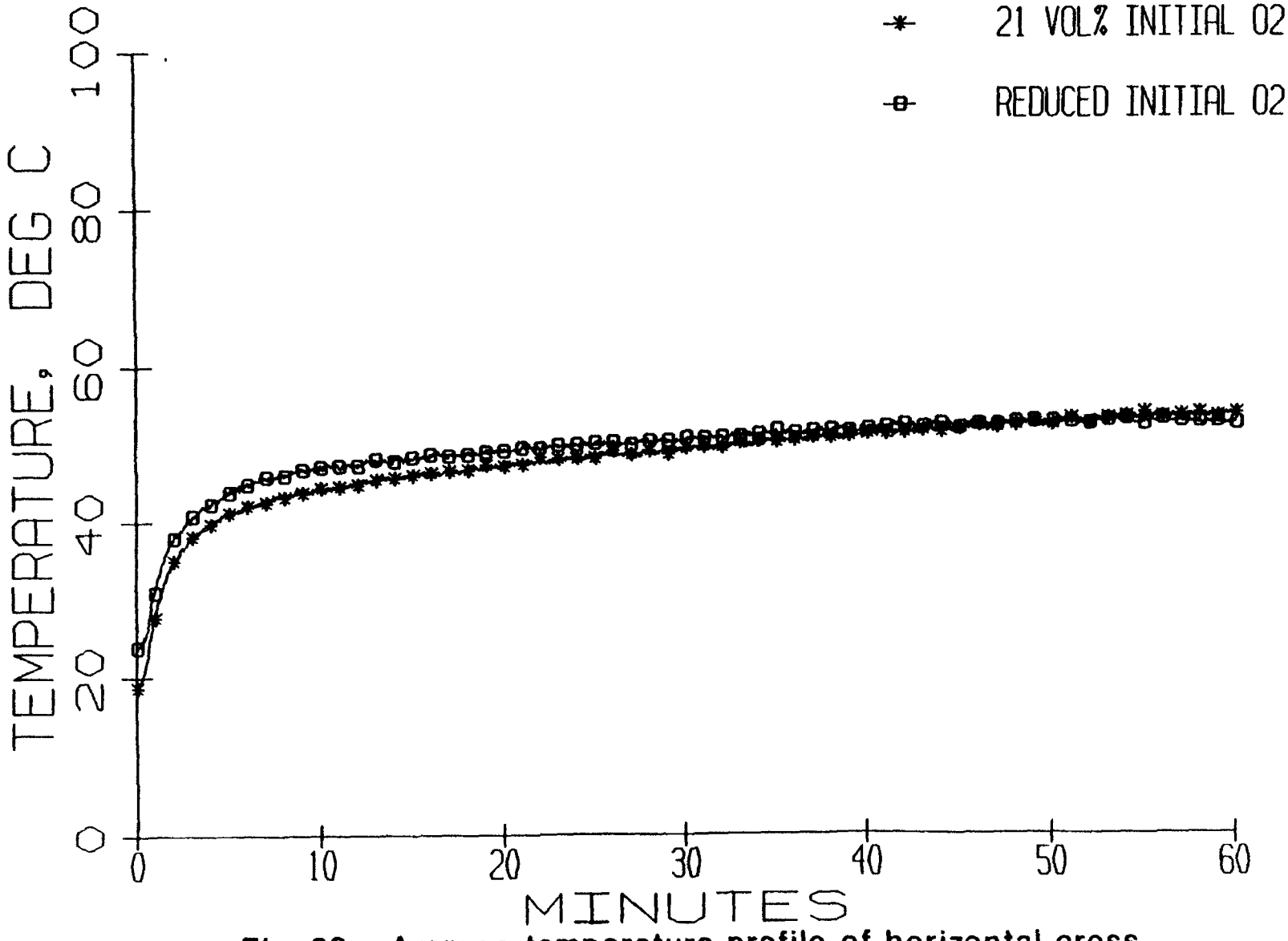

Fig. 29 - Average temperature profile of horizontal cross section approximately 3.40 m (134 in.) from lower deck

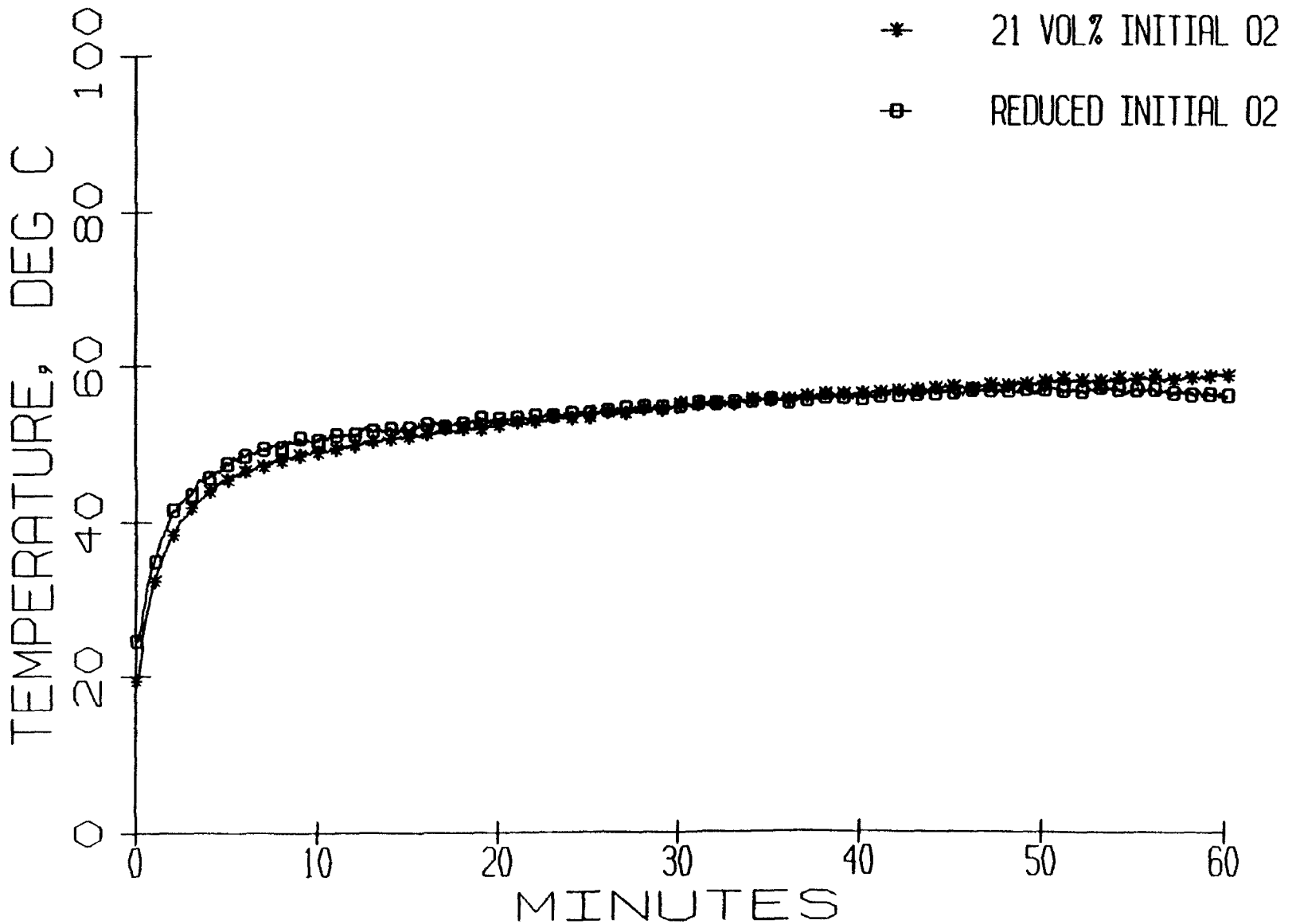

Fig. 30 - Average temperature profile of horizontal cross section approximately 4.17 m (164 in.) from lower deck

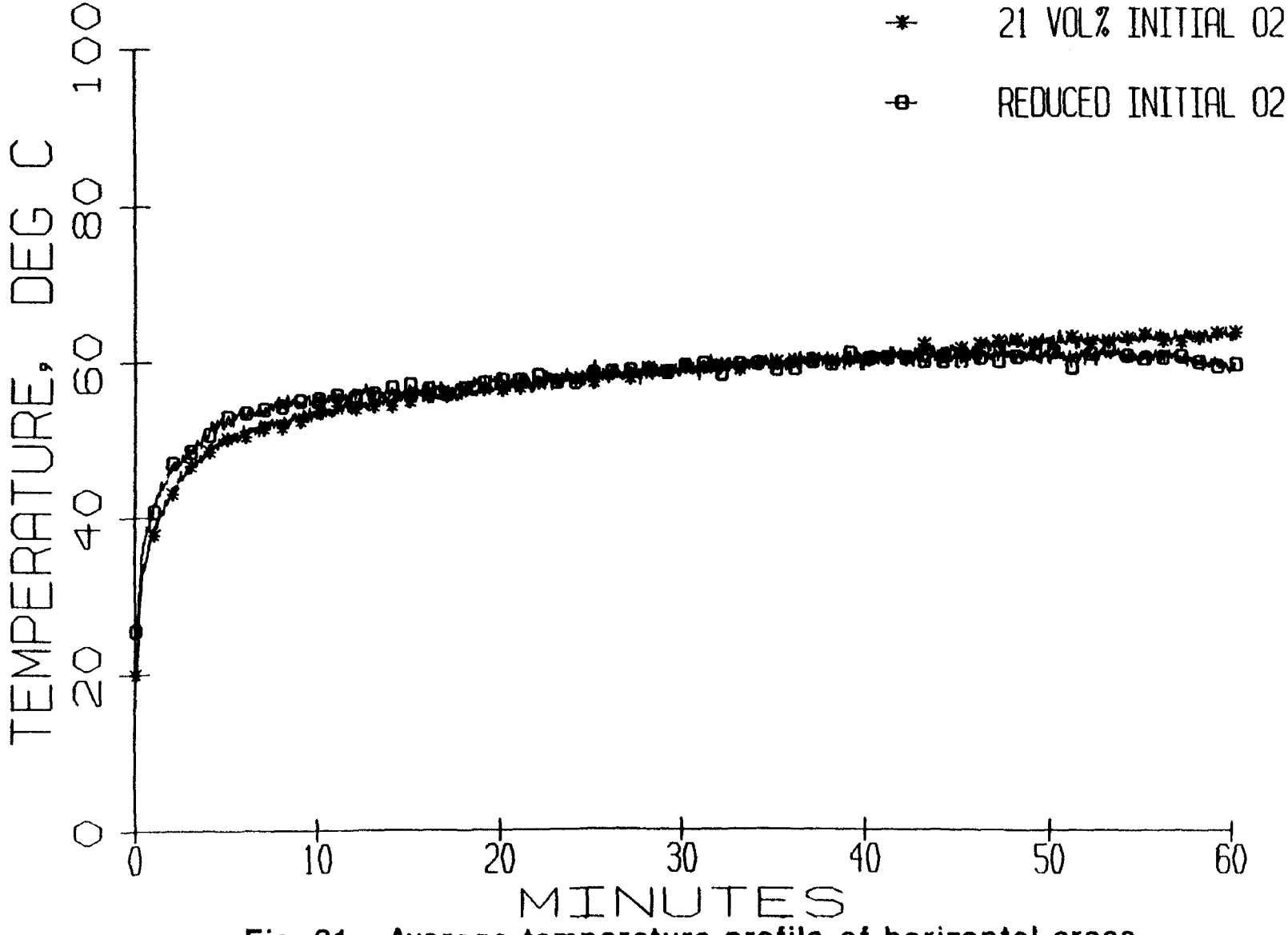

Fig. 31 - Average temperature profile of horizontal cross section approximately 4.88 m (192 in.) from lower deck

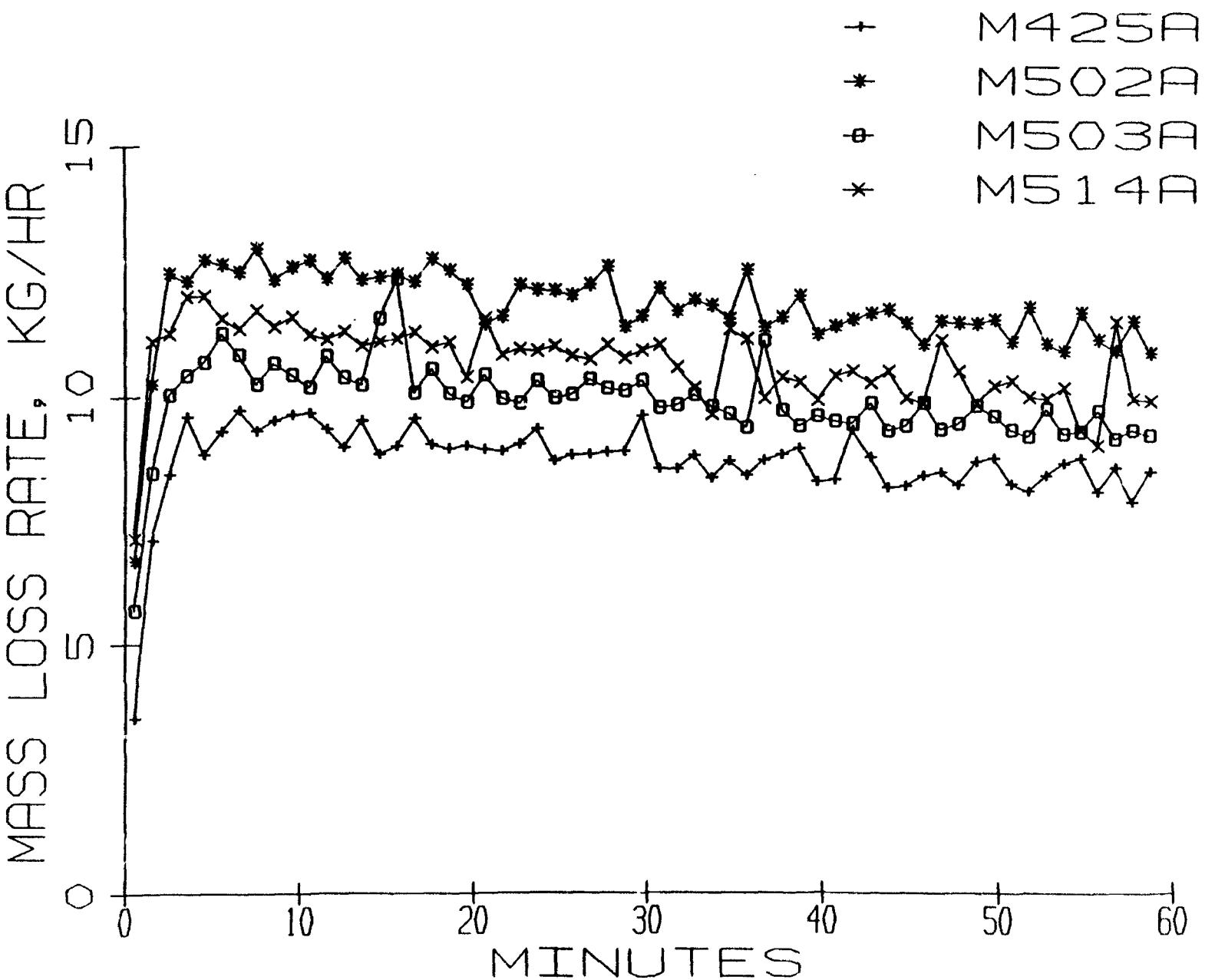

Fig. 32 - Mass loss rate of fuel at different initial chamber pressures

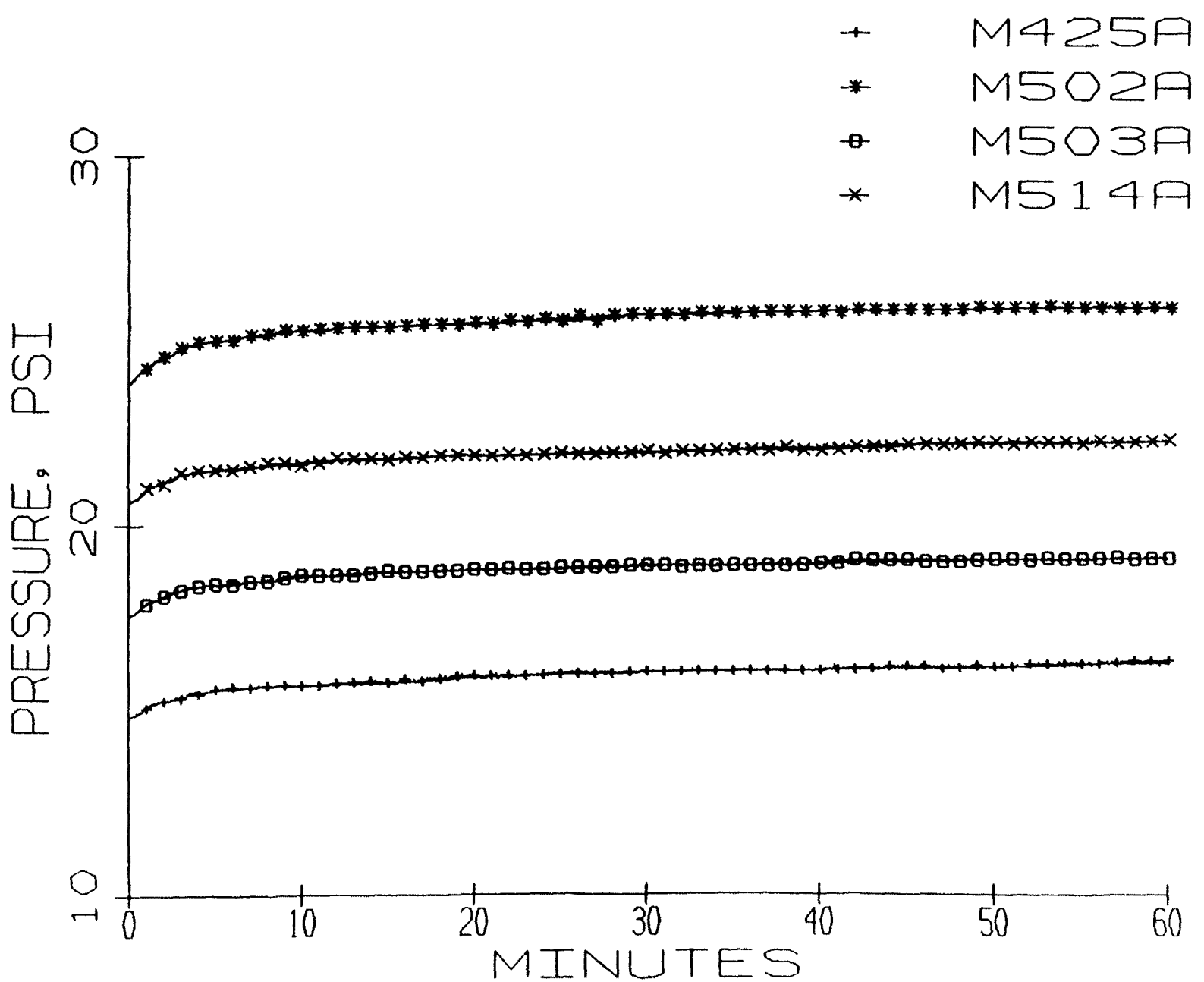

Fig. 33 - Chamber pressure profile

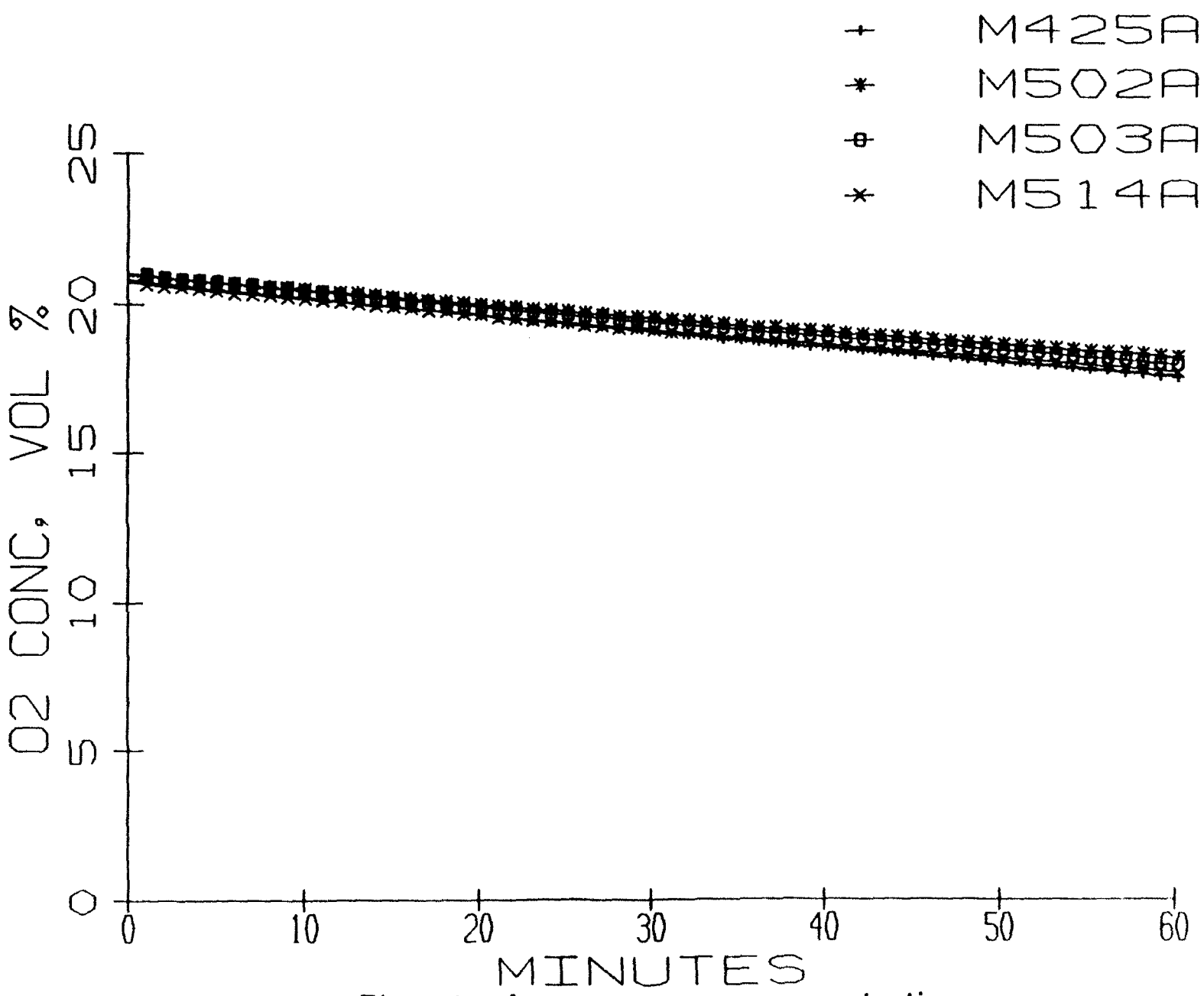

Fig. 34 - Average oxygen concentration

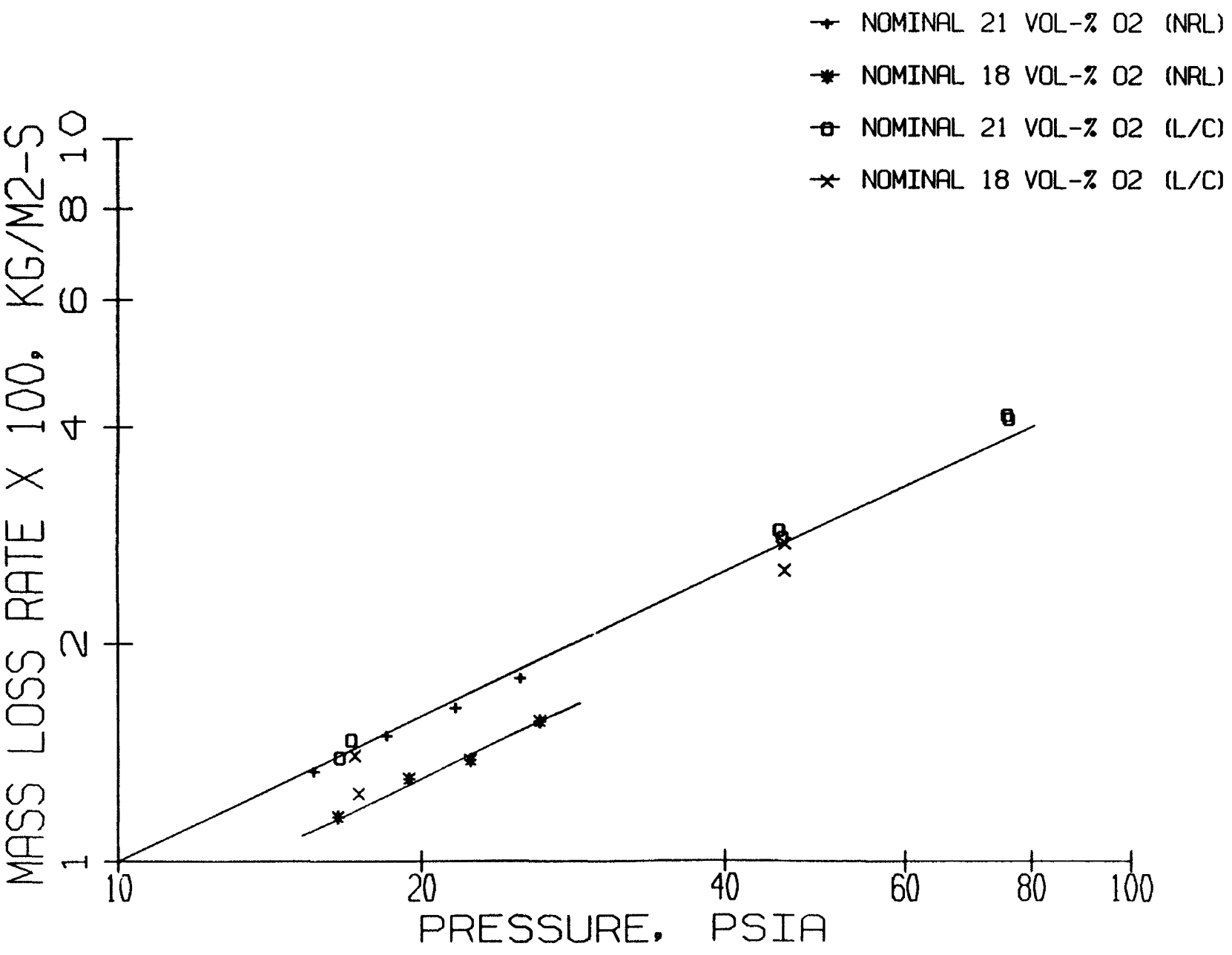

Fig. 35 - Mass loss rate of fuel as a function of pressure

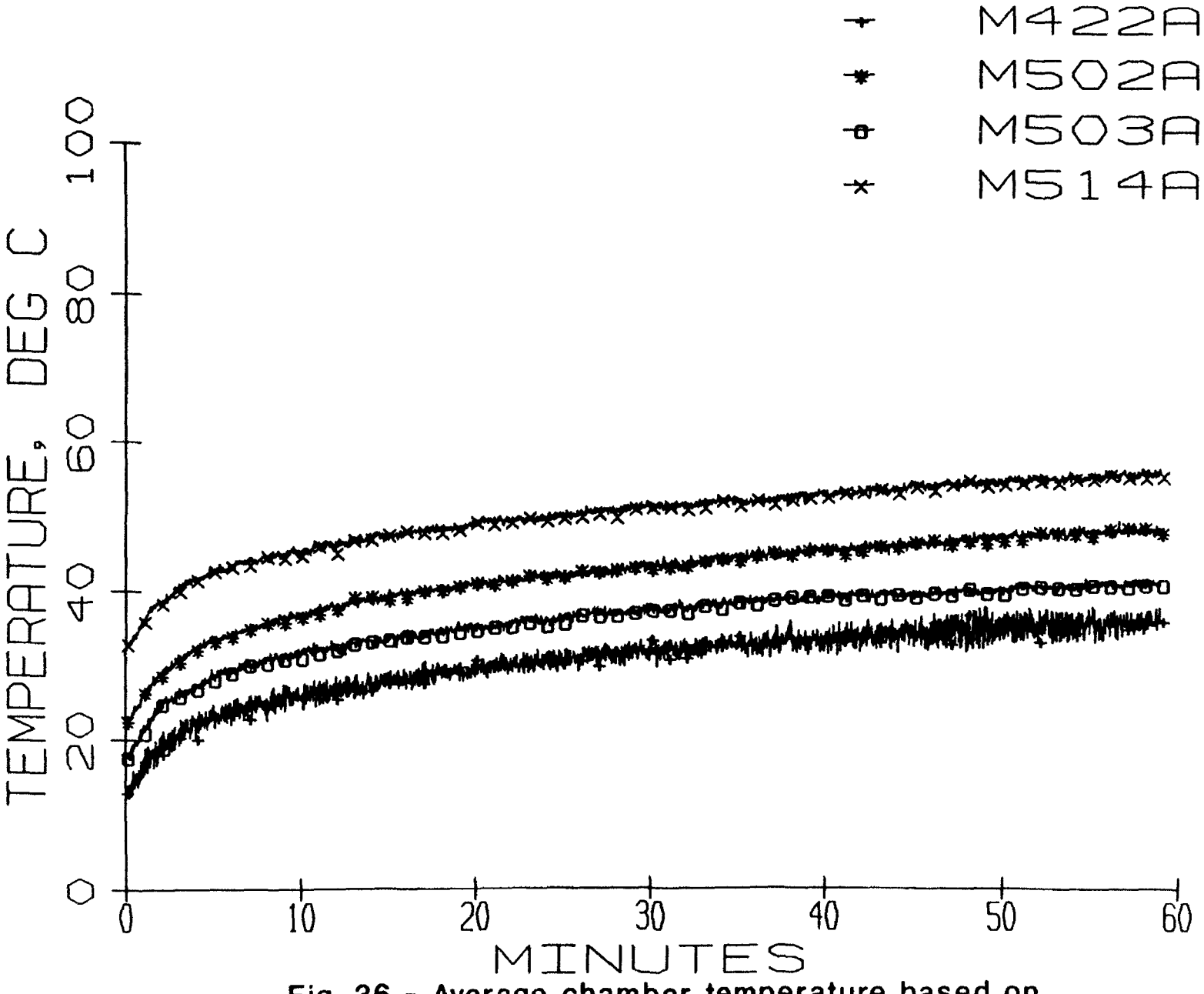

Fig. 36 - Average chamber temperature based on fwd and aft thermocouple trees

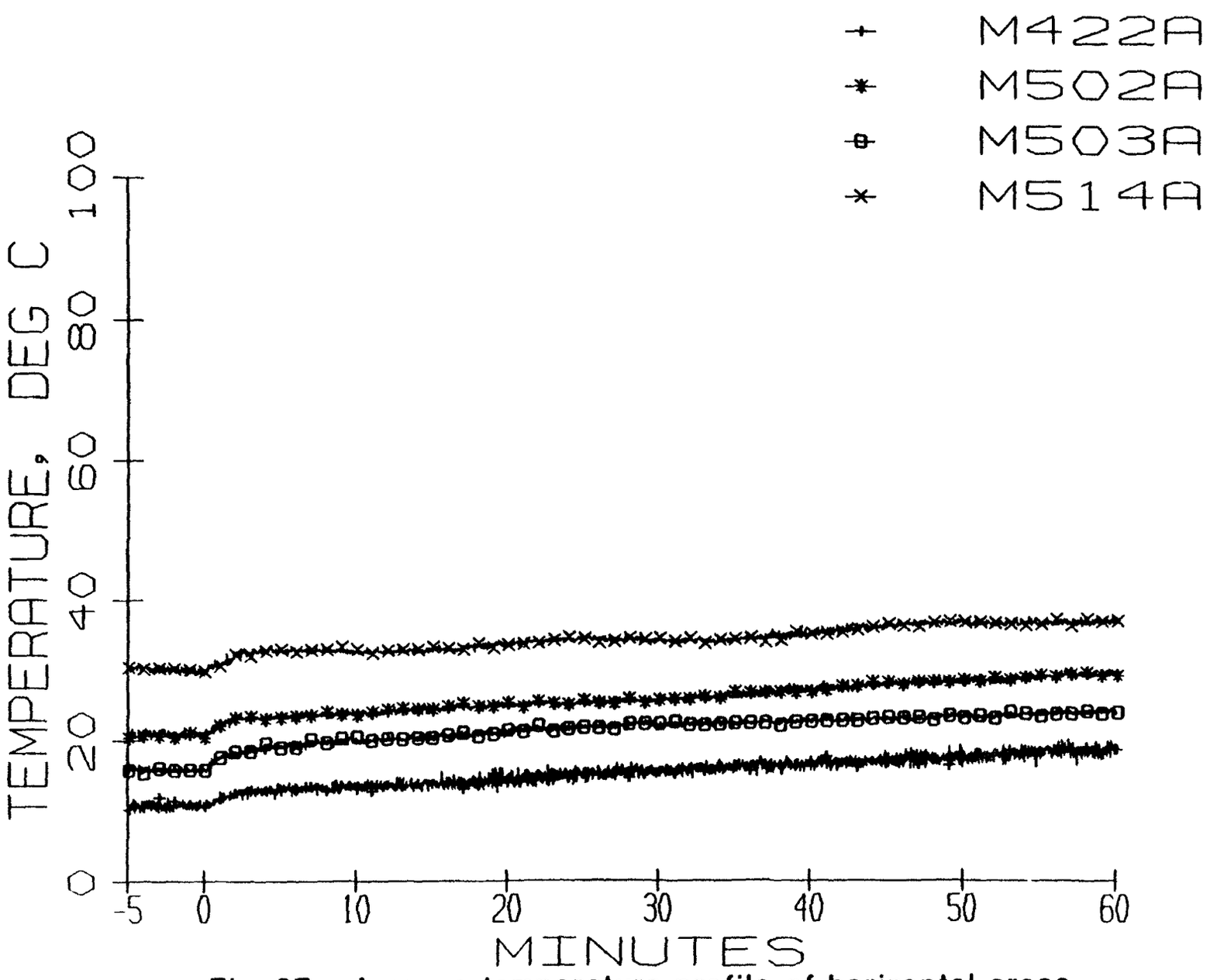

Fig. 37 - Average temperature profile of horizontal cross section approximately 0.36 m (14 in.) from lower deck

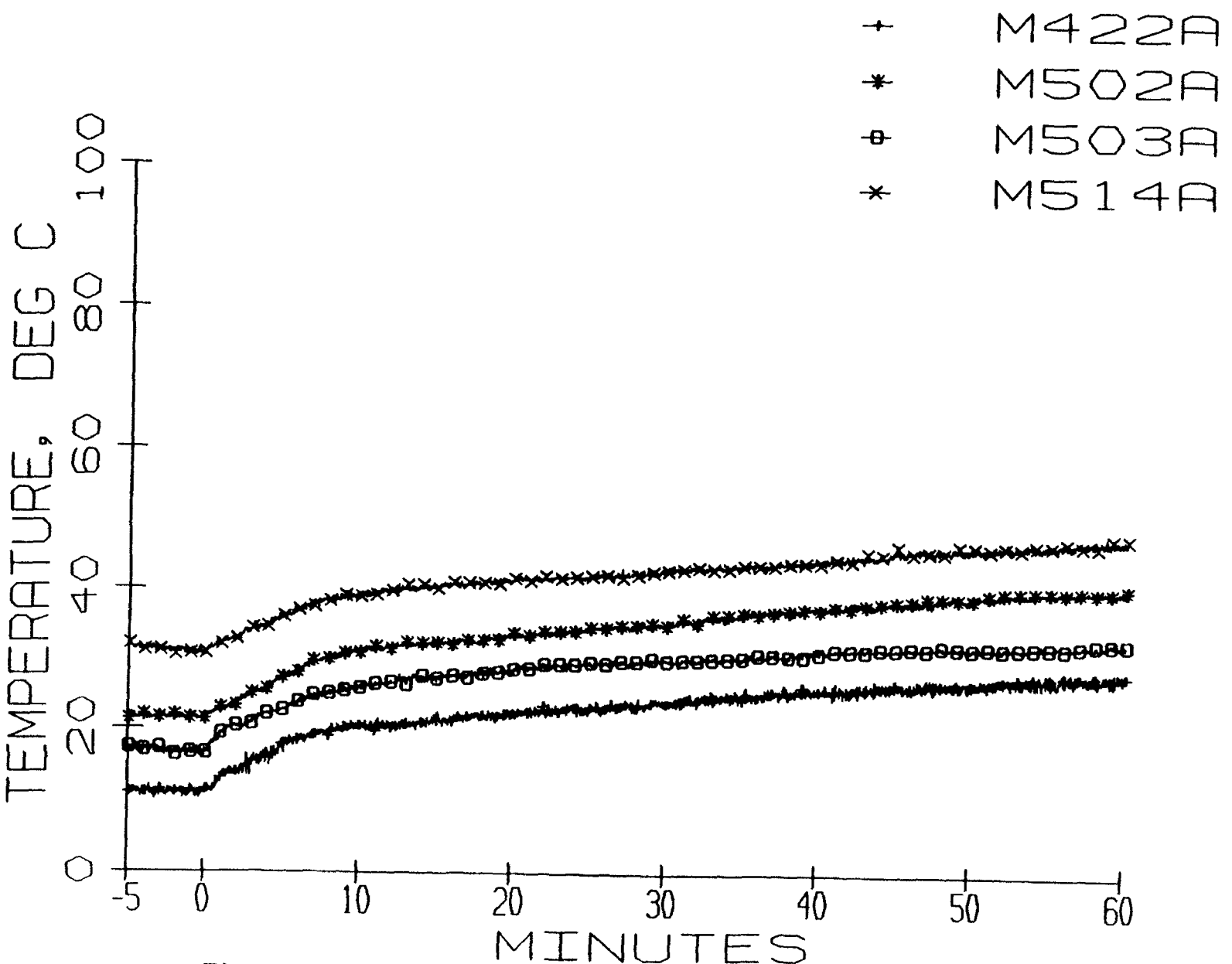

Fig. 38 - Average temperature profile of horizontal cross section approximately 1.12 m (44 in.) from lower deck

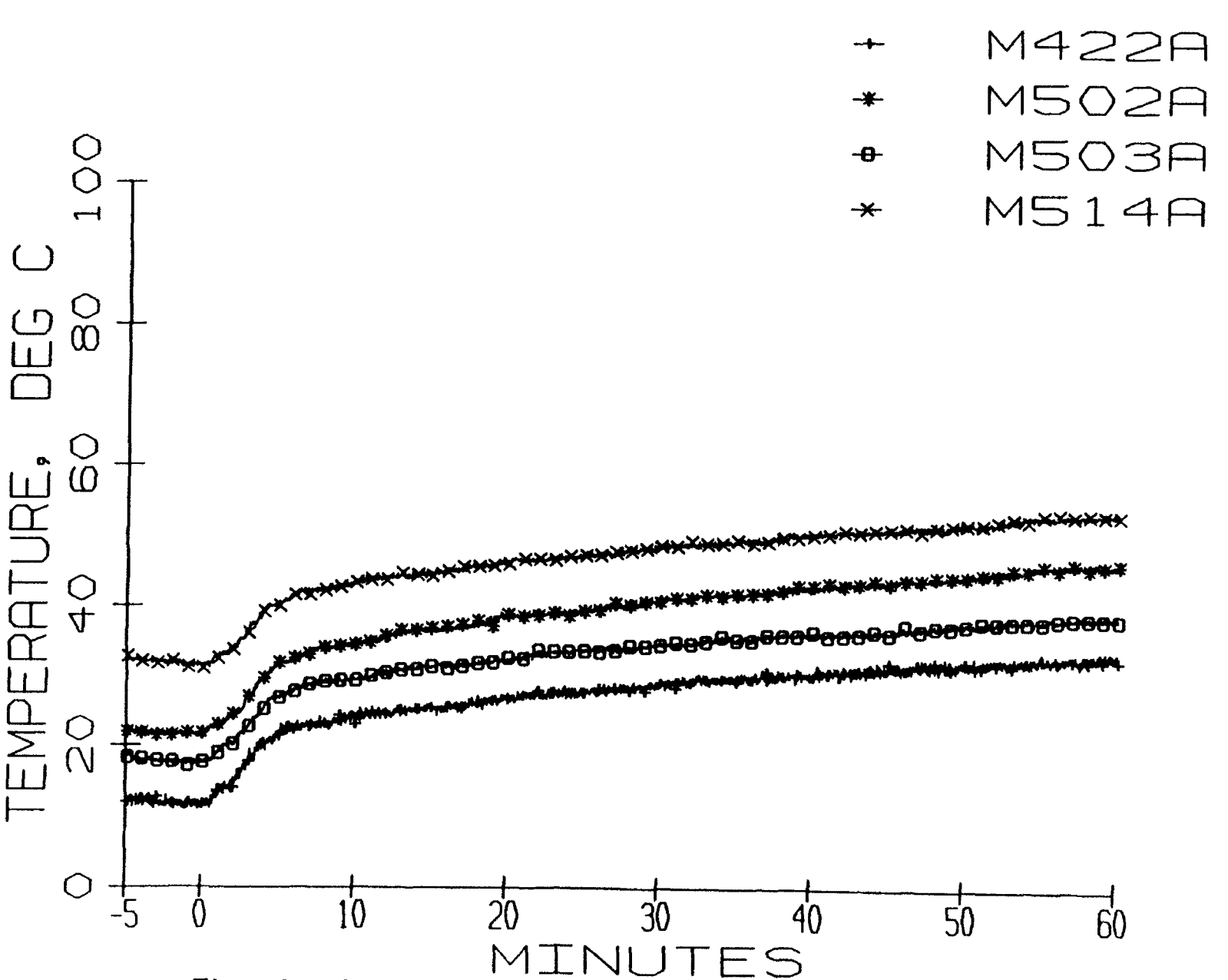

Fig. 39 - Average temperature profile of horizontal cross section approximately 1.88 m(74 in.) from lower deck

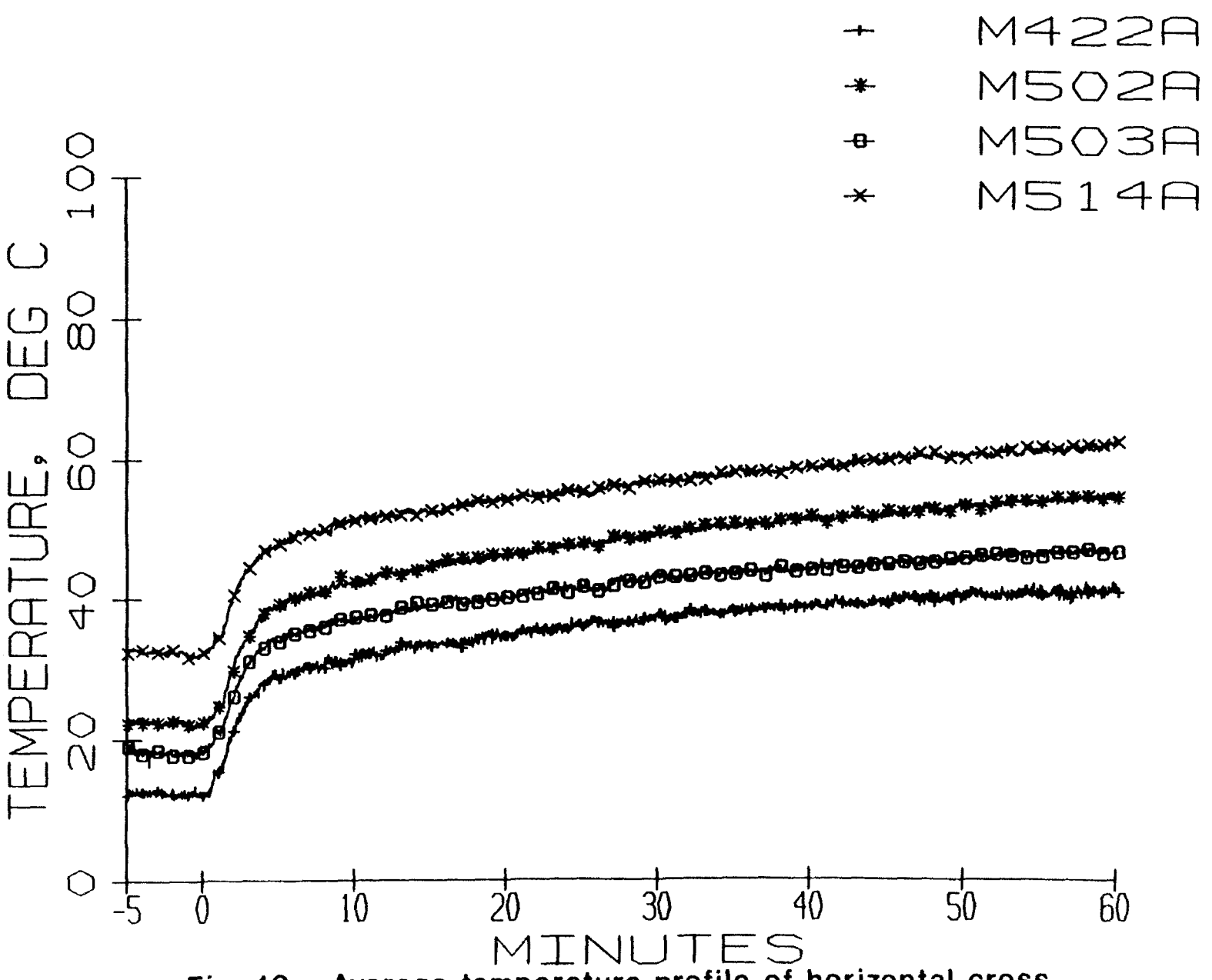

Fig. 40 - Average temperature profile of horizontal cross section approximately 2.64 m (104 in.) from lower deck

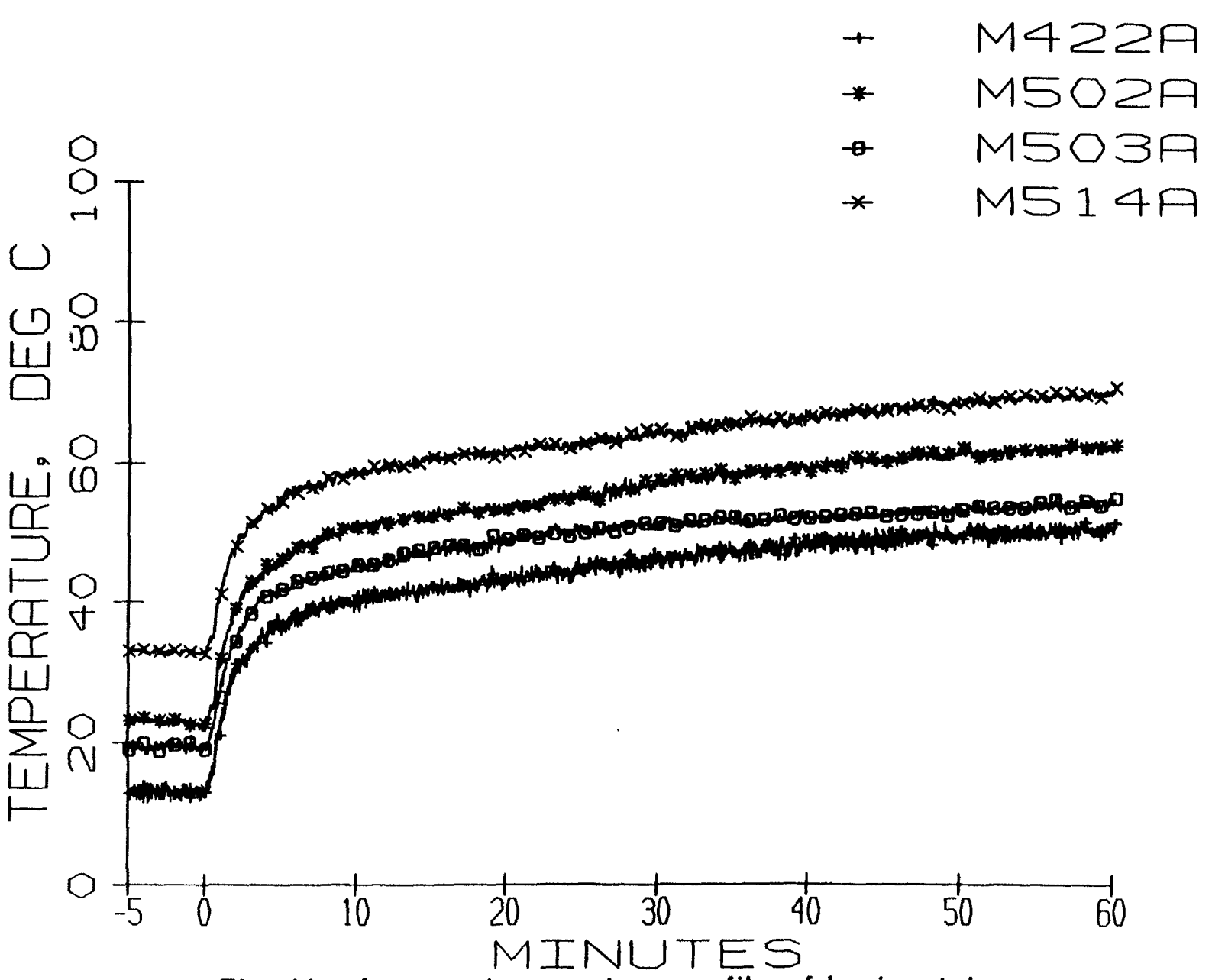

Fig. 41 - Average temperature profile of horizontal cross section approximately 3.40 m (134 in.) from lower deck

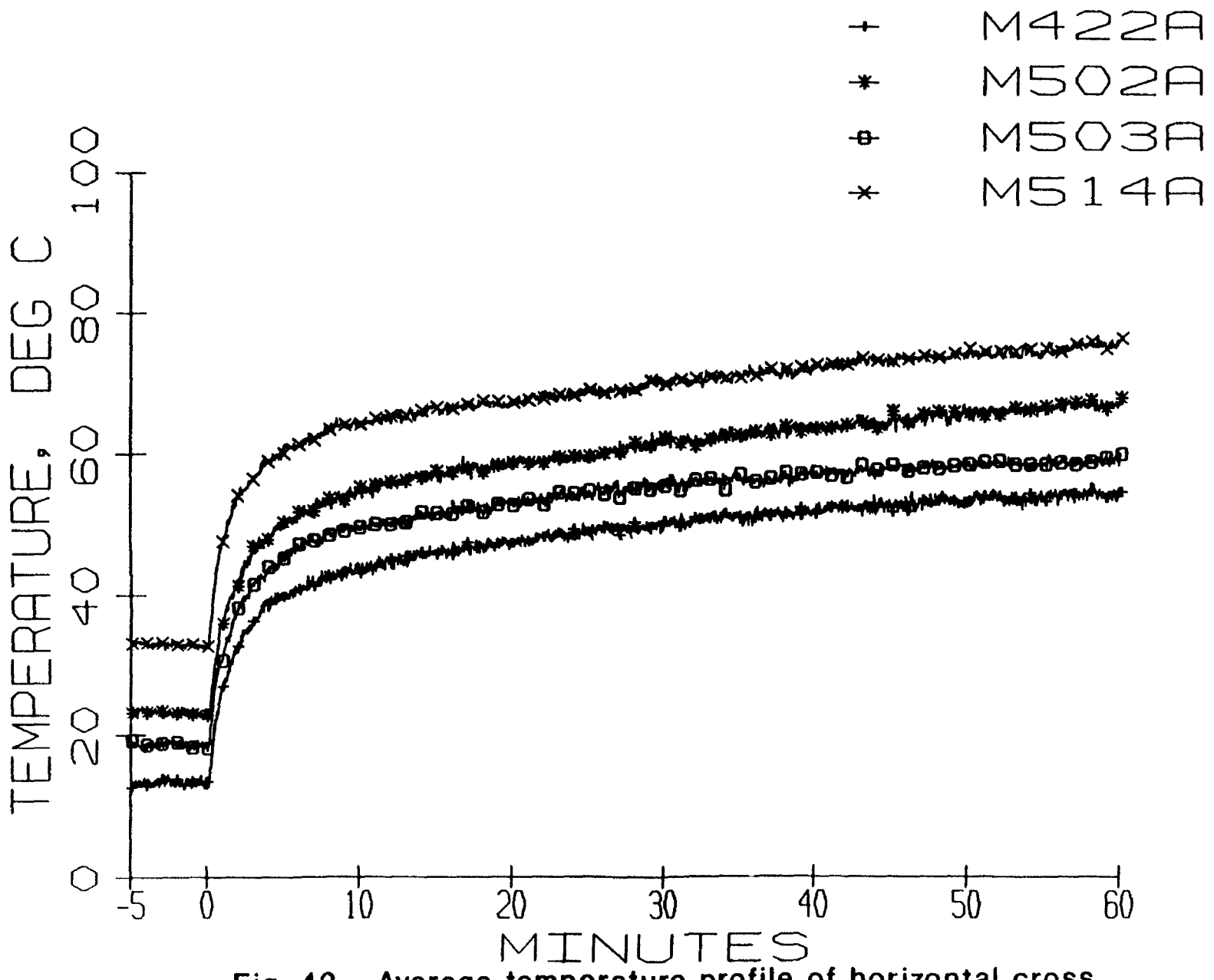

Fig. 42 - Average temperature profile of horizontal cross section approximately 4.17 m (164 in.) from lower deck

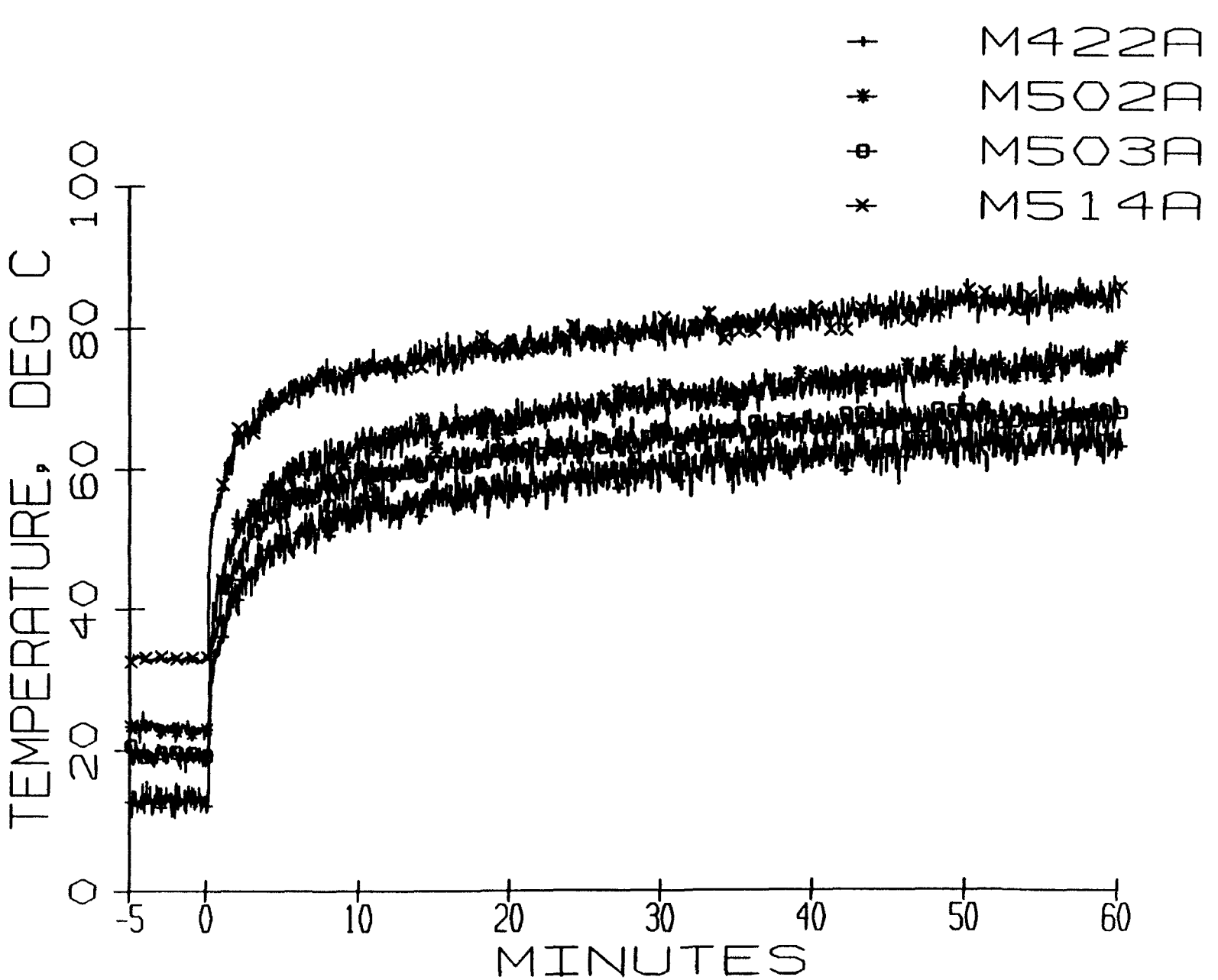

Fig. 43 - Average temperature profile of horizontal cross section approximately 4.88 m (192 in.) from lower deck

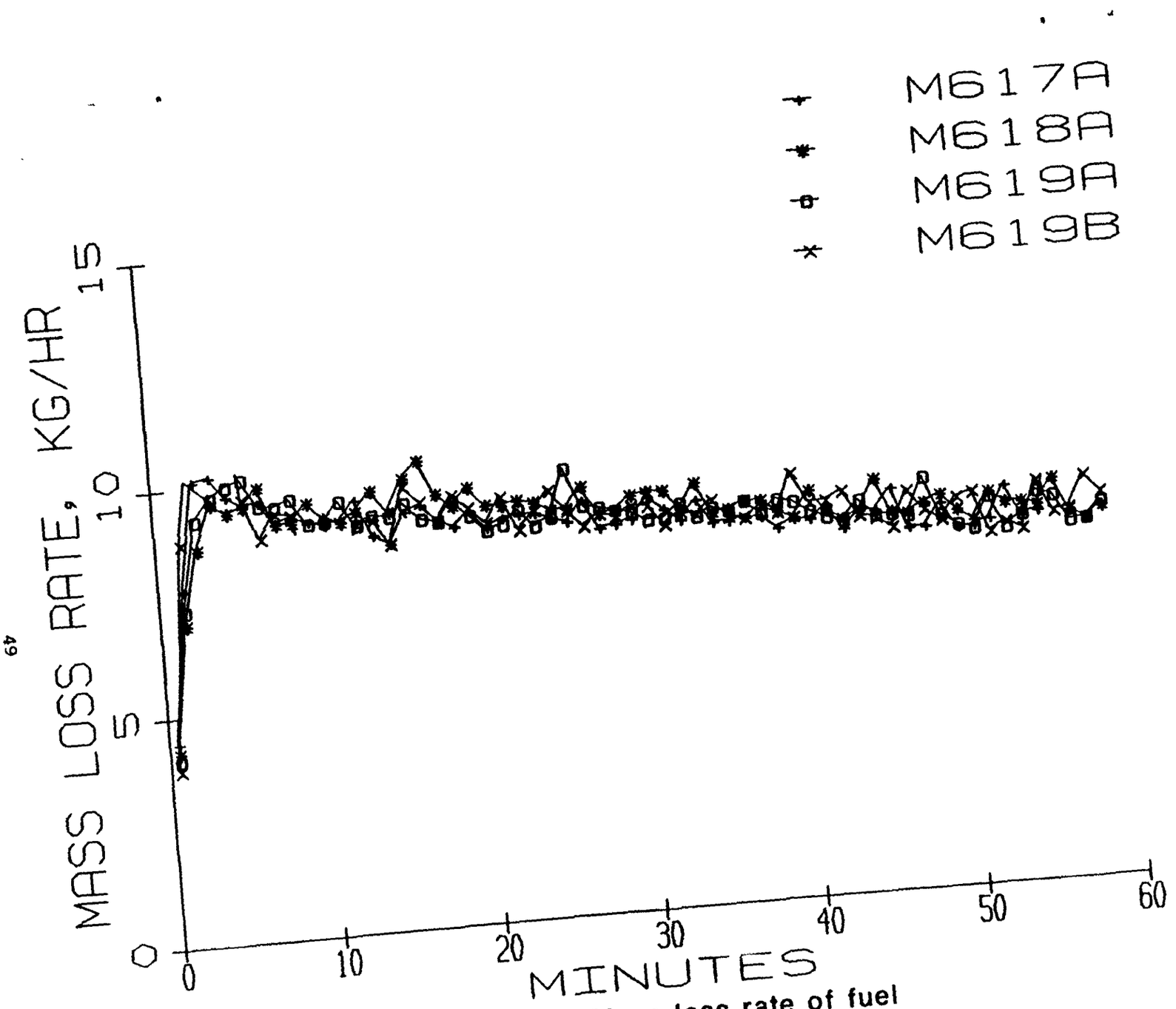

Fig. 44 - Mass loss rate of fuel

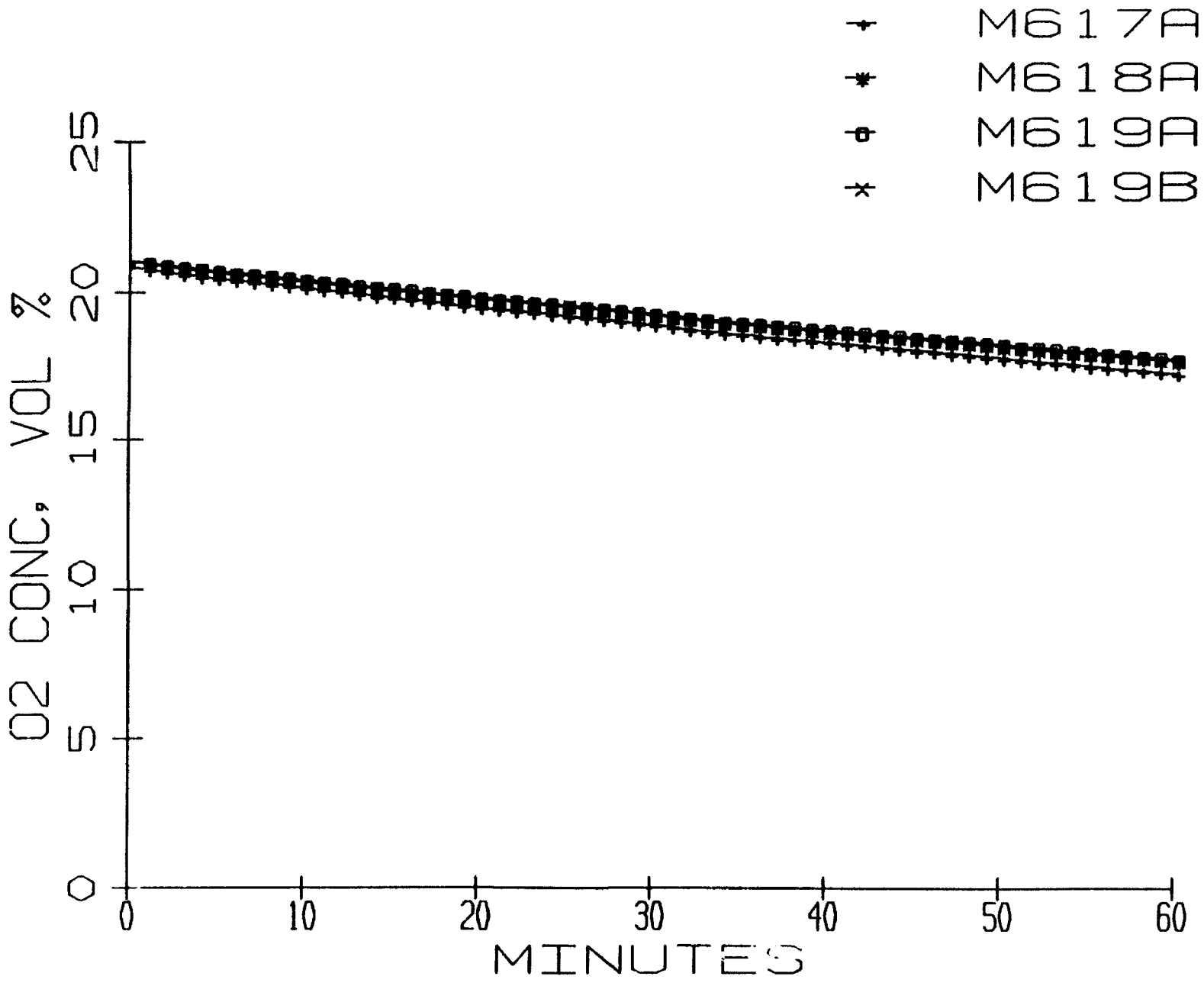

Fig. 45 - Average oxygen concentration

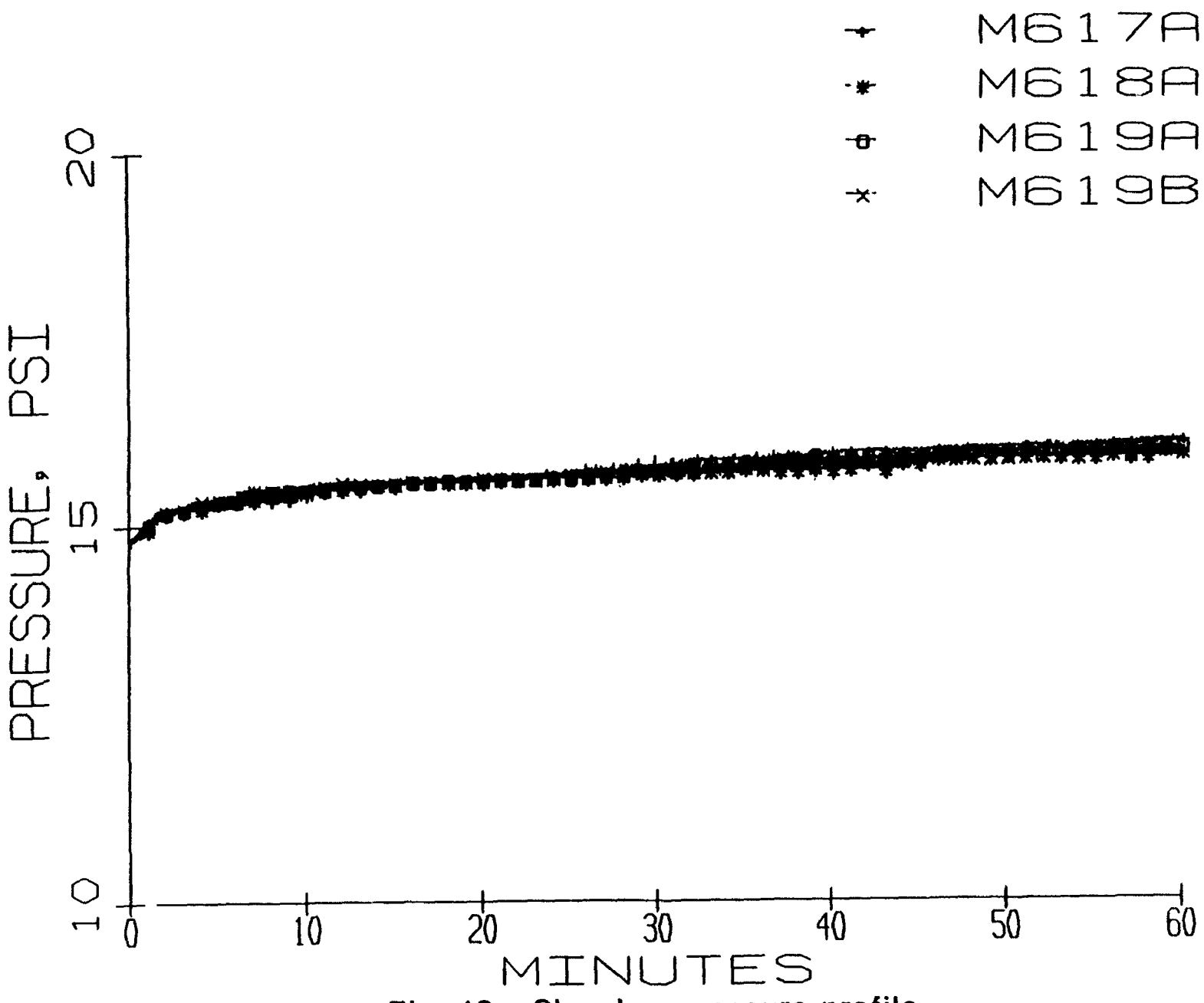

Fig. 46 - Chamber pressure profile

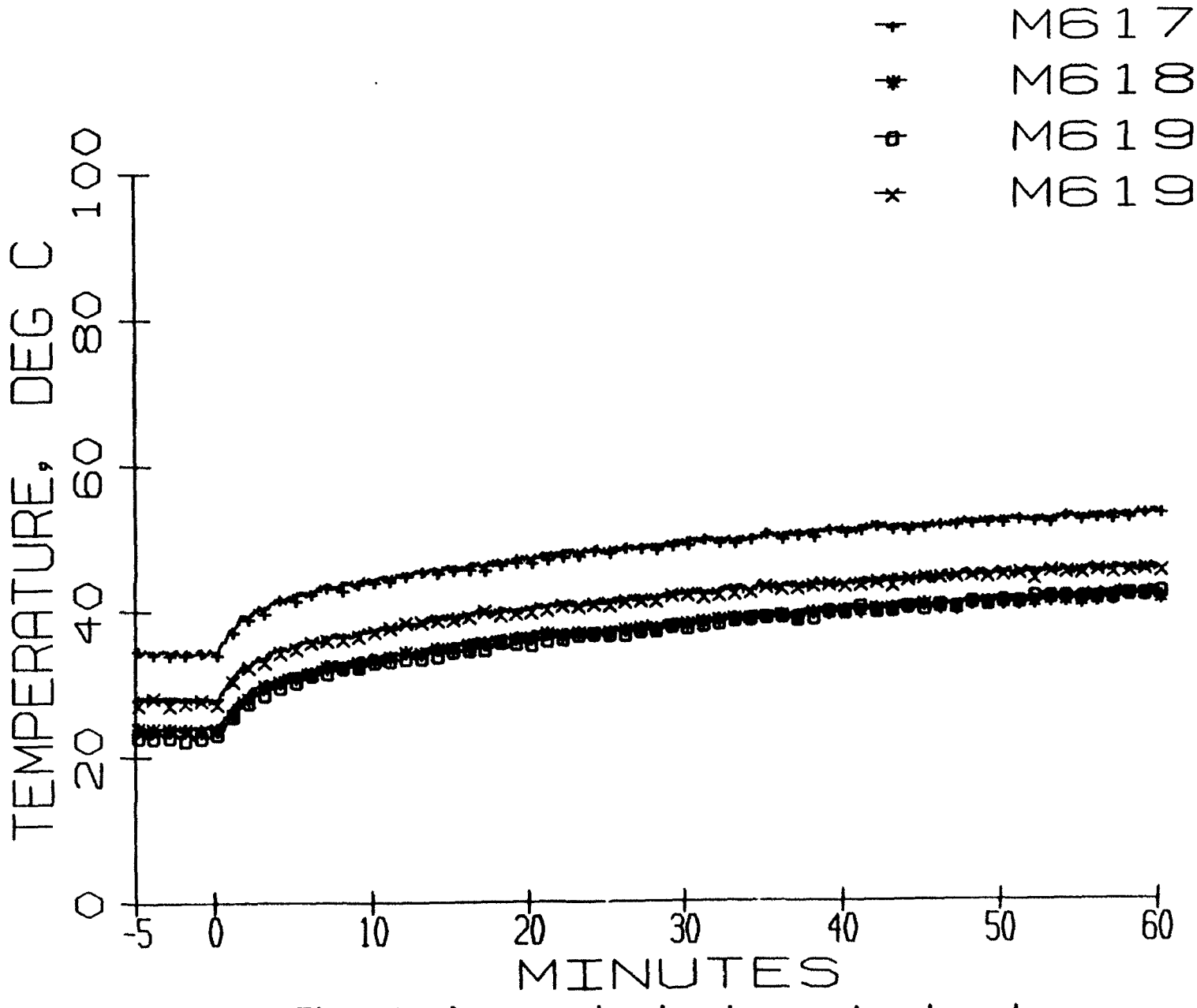

Fig. 47 - Average chamber temperature based on fwd and aft thermocouple trees